# Copyright Warning & Restrictions

The copyright law of the United States (Title 17, United States Code) governs the making of photocopies or other reproductions of copyrighted material.

Under certain conditions specified in the law, libraries and archives are authorized to furnish a photocopy or other reproduction. One of these specified conditions is that the photocopy or reproduction is not to be "used for any purpose other than private study, scholarship, or research." If a, user makes a request for, or later uses, a photocopy or reproduction for purposes in excess of "fair use" that user may be liable for copyright infringement,

This institution reserves the right to refuse to accept a copying order if, in its judgment, fulfillment of the order would involve violation of copyright law.

Please Note: The author retains the copyright while the New Jersey Institute of Technology reserves the right to distribute this thesis or dissertation

Printing note: If you do not wish to print this page, then select "Pages from: first page # to: last page #" on the print dialog screen

## ABSTRACT

## FUNDAMENTALS OF DRY COATING IN FLUIDIZED BED

by
**Rakesh Iyer**

This thesis is devoted to the study of a novel dry coating method in fluidized bed – Dry Coating of Particles in Spouted bed (DCPS). The main objectives of this work were to study the feasibility of the process, both quantitatively and qualitatively, and to compare the results with coating by conventional mechanical mixing. Aerosol mechanics is applied to account for the following: 1) collision between the guest and host particles in a spouted bed (analysis of guest-host particle inertial fluid-dynamic interaction), and 2) to show how collision efficiency of guest particles with host particles affect the coating efficiency. An equation for relating coating efficiency to collision efficiency was derived. This equation predicts high coating efficiency for large-size guest aggregates and low coating efficiency for small-size guest aggregates. The experimental results confirmed the above predictions.

It was established that large-size guest aggregates deformed during collision in the spouted bed resulting in patches over the surface of the host. This deposition mode results in large surface coverage. It was also established that the relative variation of coating among coated host particles by this method was very low. The relative variation of patches over the coated host surface was very low and from literature survey it was found that single particle coating resulted in non-uniform distribution over host particle surface [10]. Dry coating by conventional mechanical mixing was investigated and

compared with the novel dry coating method proposed in this thesis. This investigation demonstrated that coating by mechanical mixing resulted in non-uniform coating and harmful manifestation of guest particle agglomeration during the mixing process.

# FUNDAMENTALS OF DRY COATING IN FLUIDIZED BED

by
Rakesh Iyer

A Thesis
Submitted to the Faculty of
New Jersey Institute of Technology
in Partial Fulfillment of the Requirements for the Degree of
Master of Science in Chemical Engineering

Department of Chemical Engineering

May 1999

## APPROVAL PAGE

## FUNDAMENTALS OF DRY COATING IN FLUIDIZED BED

**Rakesh Iyer**

Dr. M.E. Labib, Thesis Advisor — Date
Professor, Dept. of Environmental Engineering, NJIT

Dr. Robert Pfeffer, Committee Member — Date
Distinguished Professor, Dept. of Chemical Engineering, NJIT

Dr. Rajesh N. Dave, Committee Member — Date
Professor, Dept. of Mechanical Engineering, NJIT

**This thesis is dedicated to my beloved family**

## BIOGRAPHICAL SKETCH

**Author:** Rakesh Iyer

**Degree:** Master of Science

**Date:** May 1999

**Undergraduate and Graduate Education:**

- Master of Science in Chemical Engineering,
  New Jersey Institute of Technology, Newark, NJ 07102, 1999

- Bachelor of Engineering in Chemical Engineering,
  R.V.College of Engineering, Bangalore University, Bangalore,
  India, 1995.

**Major:** Chemical Engineering

## ACKNOWLEDGMENT

Words are not sufficient to express my deepest gratitude to Dr. Mohammed Labib who provided invaluable guidance and advice throughout the course of this work. His support, encouragement, understanding and reassurance are my inspiration. I am grateful to him for providing me an opportunity to work under his supervision during my graduate study at NJIT.

My deepest gratitude to Dr. S.S. Dukhin for his invaluable guidance, ideas and advise throughout the course of this work. I am very grateful to him for his help and support.

I thank Dr. Rajesh Dave wholeheartedly for being the member of the committee and for his encouragement, ideas, support and understanding. I also thank him for allowing me to use his laboratory facilities to build my equipment and providing me with glass beads and alumina particles for carrying out coating experiments.

I thank Dr. Robert Pfeffer wholeheartedly for being the member of the committee, for his encouragement, support and understanding.

Special appreciation goes to William Dunphy for his help in building my fluidized-spouted bed. I thank whole heartedly my friends, Michelle Ramlakhan and Manish Babladi for their encouragement and support.

I wish to thank my family for their unconditional love and support, which I could not express in words and cannot repay them by any means.

Many thanks are due to my friends who helped me in various ways. Although it is not possible to name them all, their help and friendship are sincerely appreciated.

## TABLE OF CONTENTS

**TABLE OF CONTENTS**
**(continued)**

**Table of Contents**
**(continued)**

## TABLE OF CONTENTS
## (continued)

## List of Tables

## LIST OF FIGURES

## LIST OF FIGURES
## (continued)

# CHAPTER 1

# INTRODUCTION

The preparation of engineered particulates (particulates with tailored properties) is important in many industrial applications. One important class of such engineered particulates is "composite particles", specifically where one type of particles are coated onto another type. In such systems, secondary particles, referred to as guest particles, adhere to the surface of the core particles, referred to as host particles. Various inter-particle forces such as van der Waals, electrostatic and capillary forces are important in controlling the adhesion of the guest particles to the surface of host particles. In actual applications, the size of guest particles can vary from a few nanometers to greater than 1μm, while the size of the host particles can range from less than 1μm to more than 200μm.

Engineered particulates have a wide-range of applications, including: pharmaceutical products, ceramics cutting tools, phosphors for displays, food and agricultural products. In each of these applications, it is desired to incorporate a functional property at the surface that is different from that of the host core particle. To achieve this, particulates are designed so that their surface properties such as conductivity, wetability, rheology, sinterability, corrosion characteristics or flow behavior are different from the bulk of the host material. Thus, the preparation of specifically engineered "coated" particulates is important and should have major emphasis in the field of particle technology [1].

The history of coating of particles dates back to over 2000 years and date back to the Greeks and Romans, and was recorded in the drug literature of early Islam. It was not until the 19th century that drugs were coated in rotating pans. Prior to 1950's, the same types of coating pans developed in the mid-1800's were still the only feasible production method for coating pellets or tablets. Since the 1950's significant technological changes have occurred in the coating process. Notably, Wurster invented a new wet coating method for tablets and introduced the fluidized bed technology to the pharmaceutical industry. The "Wurster" process produced uniform coatings in reasonable operating times, and has set a revolutionary direction in this field. The primary advantages of fluidized bed coating process are good coating uniformity, excellent drying conditions, and flexibility to coat variety of solids substrates – mostly pellets or tablets [2]. Investigators have studied the above coating process and reported kinetic models for this process [3,4].

Coating processes can be broadly classified into two categories: namely, wet and dry coating. Dry coating is dealt with in detail in Chapter 2, however, both the types of coating are briefly described in Section 1.1.

## 1.1 Coating of Particles

### 1.1.1 Wet Coating

In a conventional wet coating process, the particles/pellets/tablets to be coated are first dispersed in an aqueous or non-aqueous liquids. Subsequently, guest particles (also made as a dispersion in liquid) are add where they are precipitated onto the surface of host

particles. This wet coating technique relies on electrostatic and van der Waals forces, and the use of binders to improve the adherence of guest to host particles [1].

In the fluidized bed wet process, the coating material usually consists of a polymeric binder, solvents (organic or water) and pigments. A mixture of two types of solvents is normally used, namely: fast solvents, which evaporate before the spray droplets reach the surface, and slow solvents which evaporate after the polymer reaches the surface. Fast solvents evaporate rapidly in the spray to deposit the coating with high enough viscosity to prevent running and sagging. The slow evaporating solvents are typically present in smaller proportion in the solvent blend and function primarily by film coalescence and leveling. Wet coating methods are extensively used in automotive topcoats and component finishing, in wood and metal furniture, in appliances and in coating of pharmaceutical drugs for controlled drug release or taste masking [5-8].

To avoid the use of organic solvents in coating processes, some investigators [5-7] proposed the use of supercritical fluids as a substitute to fast-evaporating solvents to minimize harmful environmental effects. The use of supercritical coating is difficult and is still in its infancy. In general, the process of wet coating is cumbersome due to wet and sticky conditions during coating, use of environmentally harmful toxic organic solvents and high production costs. The above limitations demand the development of new coating process and techniques. Dry coating in an excellent solution to the above problem; it is expected to be environmental friendly and cost effective.

### 1.1.2 Dry Coating

Dry coating of fine particles (guest) onto large particles (host) by various methods is presently investigated as an alternative solution to the solvent-based processes. The process of dry coating is dealt with in detail in Chapter 2.

## 1.2 Objective of the Thesis

The objective of this research is to study the feasibility of a novel dry coating technique using a particle jet stream (aerosol in a flowing gas) and a fluidized bed. This novel dry coating technique was examined by injecting an aerosol of guest particles into a spouted fluidized bed of the host particles. Several key aspects of the physics and engineering of this dry coating process are investigated in this thesis.

## 1.3 Organization of the Thesis

A brief account of the main topics of this thesis is given in this chapter. In Chapter 2, we discuss dry particle coating processes, and place emphasis on the mechanisms involved in particle coating by simple mixing of the powders. We also provide an overview of inter-particulate forces, present coating results by simple mechanical mixing, fluidization of particles in spouted bed, powder de-aggregation in an orifice, and define coating quality. In Chapter 3, we present our development of a theoretical description of the process of inter-particle collision, particle sedimentation, and specifically derive the relation between coating and collision efficiencies; in the light of aerosol mechanics. In Chapter 4, we present and discuss the experimental set up and procedures. In chapter 5, we present the experimental results and provide an interpretation of such results. In Chapter

6, we present the conclusions of this work and make recommendations for future research work.

# CHAPTER 2

# DRY COATING OF PARTICLES

## 2.1 Introduction

Dry coating is a process by which a layer of fine guest particles is deposited onto the surface of larger host particles without the use of solvents. Dry coating of particles by various methods are presently being explored by others [9].

Various dry coating processes have been developed. Hiroyuki-Kage et al. [10,11] demonstrated a coating technique in a fluidized bed by atomizing the guest particles; however, the process was not completely dry due the use of a liquid binder during the process. A mixture of fine powder and binder solution is atomized with the goal of coating the fine powder onto the surface of fluidized host particles. Coating of particles in a tumbling fluidized bed by atomizing the slurries of clay particles was also studied by Abe, Hirosue and Yamada [12]. Few studies on this apparatus have been done and hence very little information has been published in this regard [12]. Based on our literature searches, little or no work has specifically addressed the area of dry coating in fluidized beds.

Mixing of guest and host particles remains to be the main method to achieve dry coating of particles. Recently, Magnetically Assisted Impaction Coating (MAIC) has been developed as dry powder coating method. In the MAIC process, magnetic beads are mixed with the host and guest particles, and are accelerated in a chamber using a specially configured magnetic field (Figure 2.1). Upon imposing of the field, magnetic beads collide with the guest and host particles to accomplish the coating [1,9].

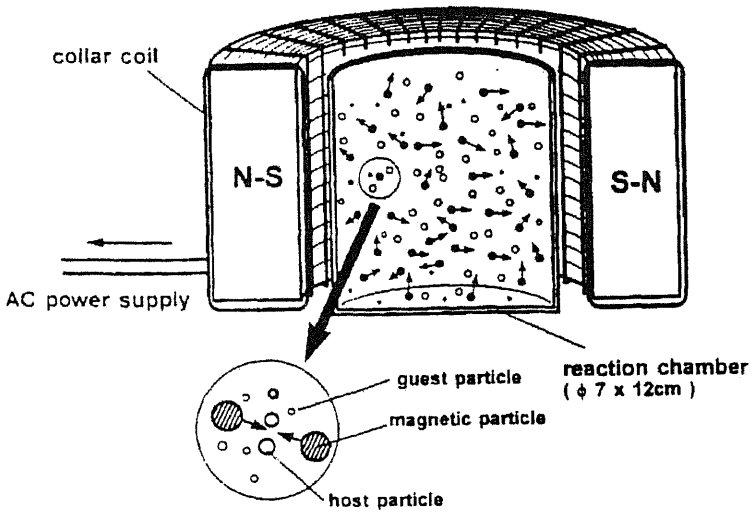


**Figure 2.1** Schematic diagram of MAIC [1,10]

Another dry mixing-coating technique proposed by Honda et al. [13,14], is effected by mechanical impact blending of powder mixture to prepare coated composite particles. In the latter, the powder is fed at the center of an impact type apparatus and the process is referred to a "hybridization" (Figure 2.2). During the process the powder is blown off in peripheral direction by the centrifugal force generated by a rotor rotating at high speed - rotation speed over 10,000 rpm. The dispersed particles hit the rotating striking pins at this high speed. Consequently, the powder receives mechanical impact on its surfaces and is efficiently blended. The powder reaching the periphery re-enters the machine through a circulation route.

In brief, dry coating techniques by conventional mixing (tumbling) requires long processing time and is limited to processes not requiring high coating quality. In the present research, coating by simple mechanical mixing was investigated and compared with our fluidized bed coating - see Section 2.2.

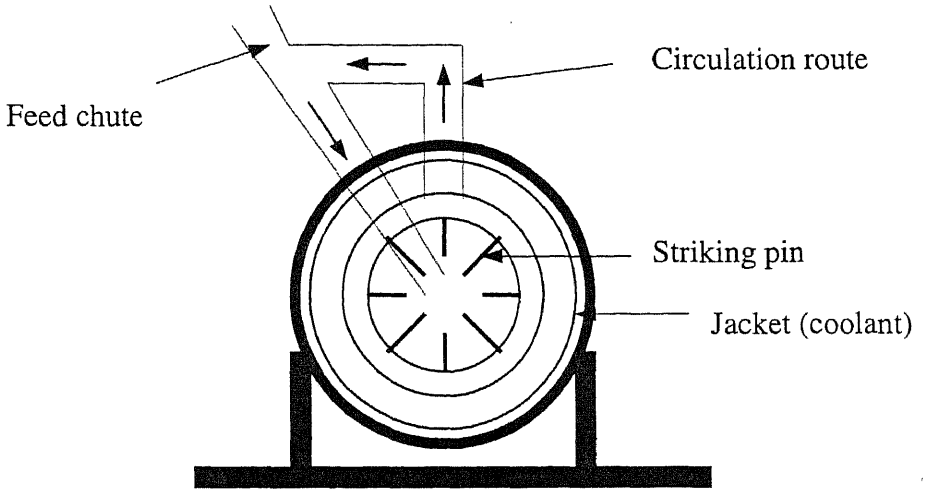


**Figure 2.2** Schematic model of Hybridizer (Adopted from Reference 13,14)

## 2.2 Dry Coating by Simple Mixing Process (DCSMP)

### 2.2.1 Mechanism

In a typical dry coating mixing process, a free-flowing coarse granular material is mechanically mixed with a fine cohesive powder - i.e., aggregated by cohesive forces. The resulting mixture is expected to have a layer of fines (guest particles) adhering to the surface of large particles. This process is referred to either as "Powder Coating" or "Ordered Mixture". Two fundamental processes take place inside the mixer:

1. Transport of groups of particles from one region of the mixer to another called "Convective" mixing, and
2. Random motion of individual particles relative to one another, called "Diffusive" mixing.

During the latter process, compaction of loose guest particles and coating of guest onto the surface of the host occurs. Compaction occurs due to the cohesion between guest

particles and coating occurs due to adhesion between guest and host particles. During the DCSMM process, large aggregates of guest particles deform between the host particles, de-aggregate and partially or wholly stick to the surface of the host particles, thereby coating them. If cohesion between the guest particles is stronger than their adhesion with host particles, compaction is favored, and the result is guest particles agglomerate formation and poor coating. As long as the component powders differ in size, shape or density, mixing or de-mixing takes place; and if the process is prolonged, an equilibrium between mixing and segregation is reached where the quality of the mixture remains unchanged. As a general rule, guest particles become segregated from the host if they are free flowing [15].

There are two regimes in dry coating, namely: primary coating and secondary coating. Primary coating occurs due to adhesion between free guest particles and surface of host particles. Secondary coating occurs due to exchange of coating material from one coated host particle to another. Secondary coating exchange (SCE) may occur either between a coated and an un-coated host particles, or between two coated host particles. Primary and secondary coating regimes occur simultaneously during the coating operation.

In the present work, the host particles used were 500μm glass beads and the guest particles were aggregated alumina of primary size particle/aggregate 0.7μm. The Glass beads had a smooth surface and were free flowing. The alumina particles had the tendency to agglomerate and were not free flowing, as it is the case with many micron-sized powders. We found that under various conditions, the DCSMM process results in a

highly non-uniform distribution of coating among host particles and that alumina forms loose agglomerates.

### 2.2.2 Coating Results by DCSMM Process

The Figures 2.3 through 2.6 are microphotographs of host glass beads coated with guest alumina by the simple mixing process. There is a high degree of non-uniformity of coating among host particles, i.e., some particles are well coated while others are not at all coated. Moreover, guest particles are present in the form of agglomerates and are dispersed among host particles.

It was found that the coating is highly non-uniform during short processing times and appear to get better around 5 minutes. However, after 5 minutes of mixing, the coating distribution among various host particles was still non-uniform and inefficient. For prolonged mixing times, the coating quality deteriorated due to the loss of guest particles from the coating layer and also due to the segregation of agglomerated guest particles. Based on these, it was found that:

1. There is a manifestation of compaction of guest particles due to collision of host particles, and there was large number aggregates of guest particles in the final mixture.
2. The guest powder segregated and formed agglomerates during long processing times.
3. The high degree of non-uniformity of coating among host particles was confirmed; This may be due to improper contact between the host and guest particles during the mixing process.

The drawbacks prompted us to explore novel dry coating techniques where two objectives were achieved as follows:

1. To overcome the agglomeration of guest particles, we proposed to de-aggregate them by rapidly de-pressurizing their aerosol through a nozzle, and
2. To overcome the disadvantageous contact between the guest and the host, we proposed to coat the host particles in a fluidized bed under controlled conditions.

During our development we explored this method of dry coating, and studied how the interaction between guest and host particles leads to coating. We studied the coating efficiency and quality as a function of process parameters. No binders were used in our work, since our objective was to study dry powder coating without interference of other variables. The results and discussion of this effort are presented in Chapter 2.2.2.

In this Chapter, powder de-aggregation is discussed in Section 2.3, coating in fluidized bed in discussed in Section 2.4 and particle collision in spouted bed is discussed in Section 2.5.

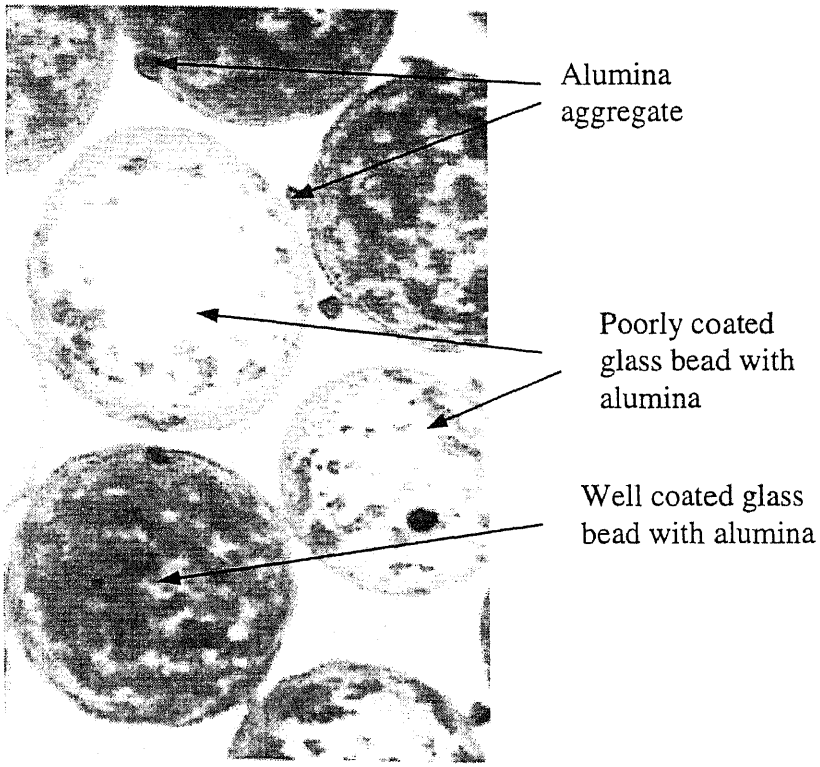


**Figure 2.3** Optical microphotograph of DCSMM process for 5 minutes: Alumina = 1g, Glass beads = 5g. **Observation**: High degree of non-uniformity of coating of alumina coating over glass beads and formation of alumina aggregates

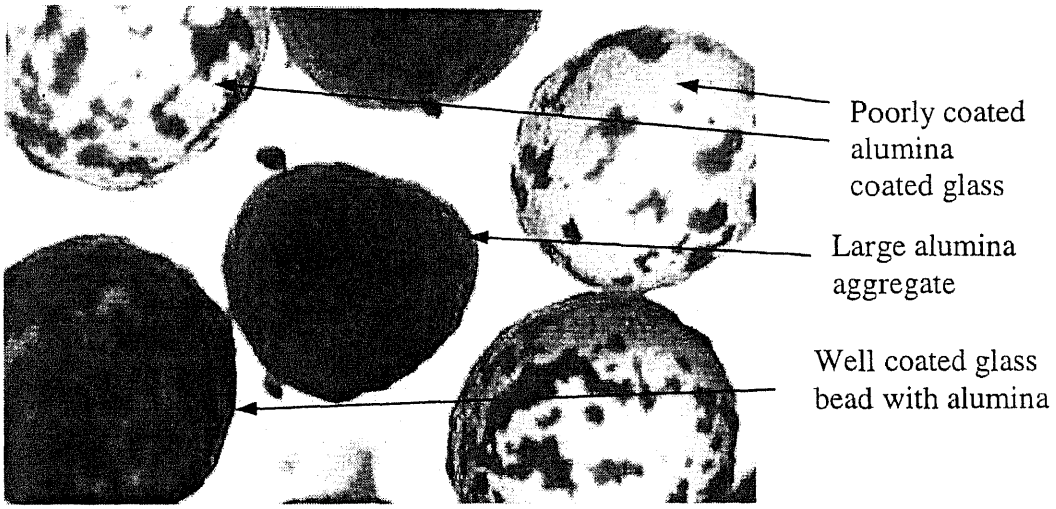


**Figure 2.4** Optical microphotograph of DCSMM process for 2 hours: Alumina = 1g, Glass beads = 5g **Observation:** Some particles are well coated and some are poorly coated, and compaction of alumina is manifested by formation of large aggregates.

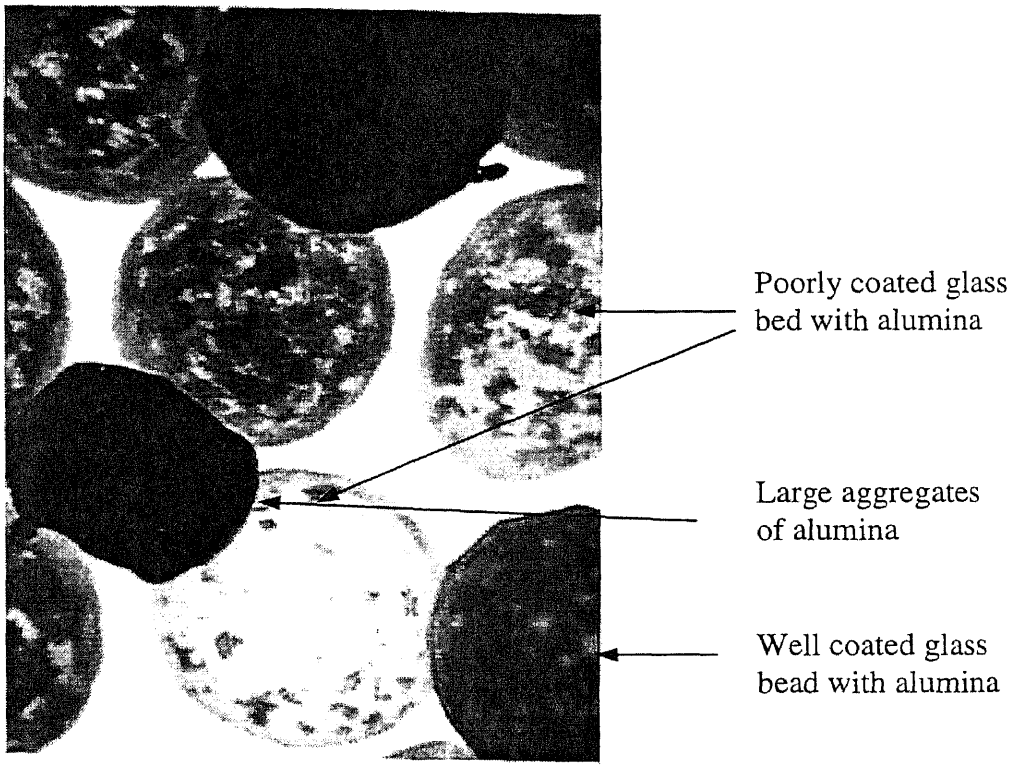


**Figure 2.5** Optical microphotograph for DCSMM processm for 5minutes, Alumina = 1g, Glass beads = 5g. **Observation:** Coating distribution became slightly better compared to other processing times, however there was manifestation of non-uniformity of coating of glass beads and compaction of alumina particles.

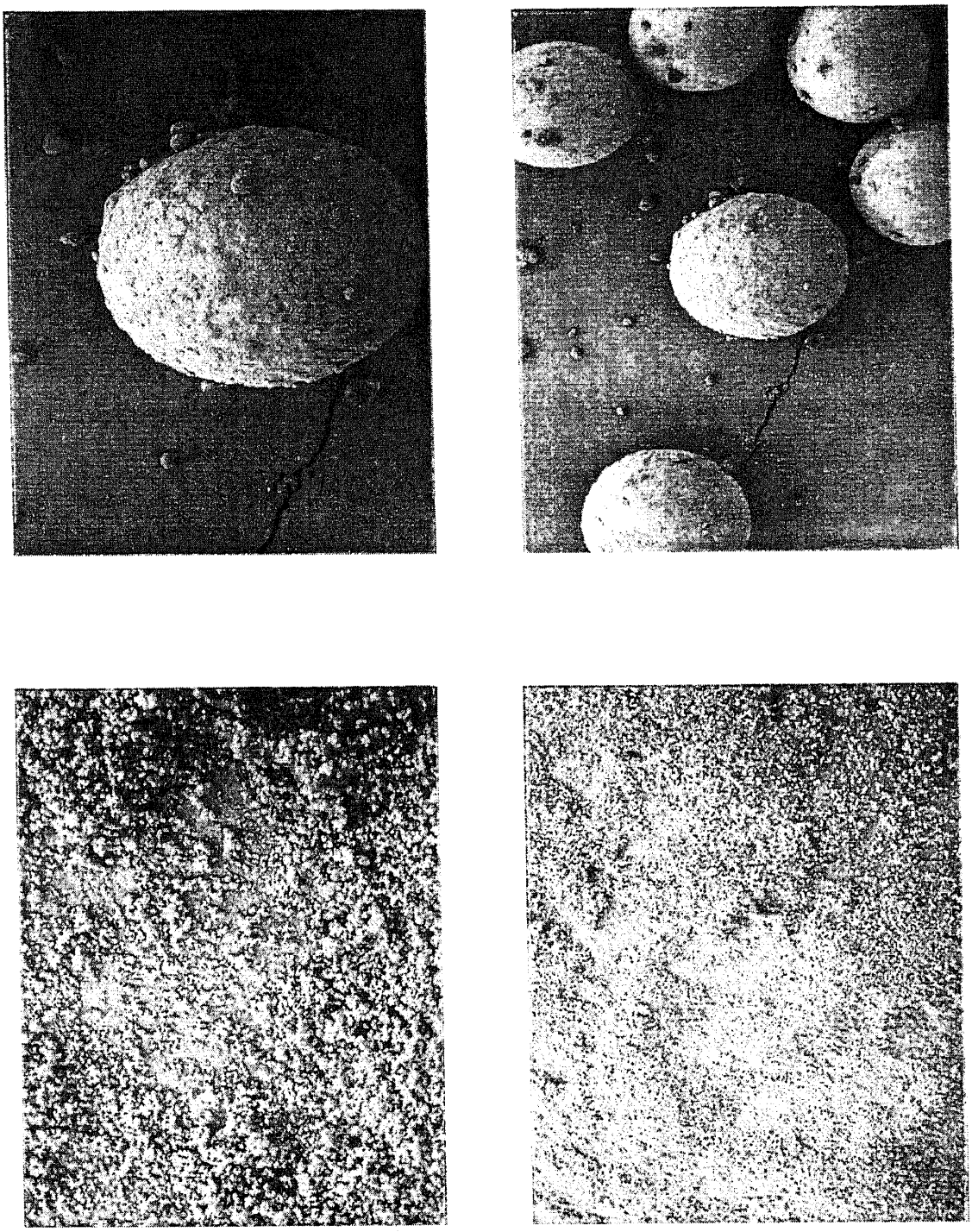

**Figure 2.6** SEM photograph of DCSMM process for 5 minutes: Alumina = 1g, Glass beads = 5g. **Observation:** Surface coverage is good, however there is formation of agglomerates of alumina.

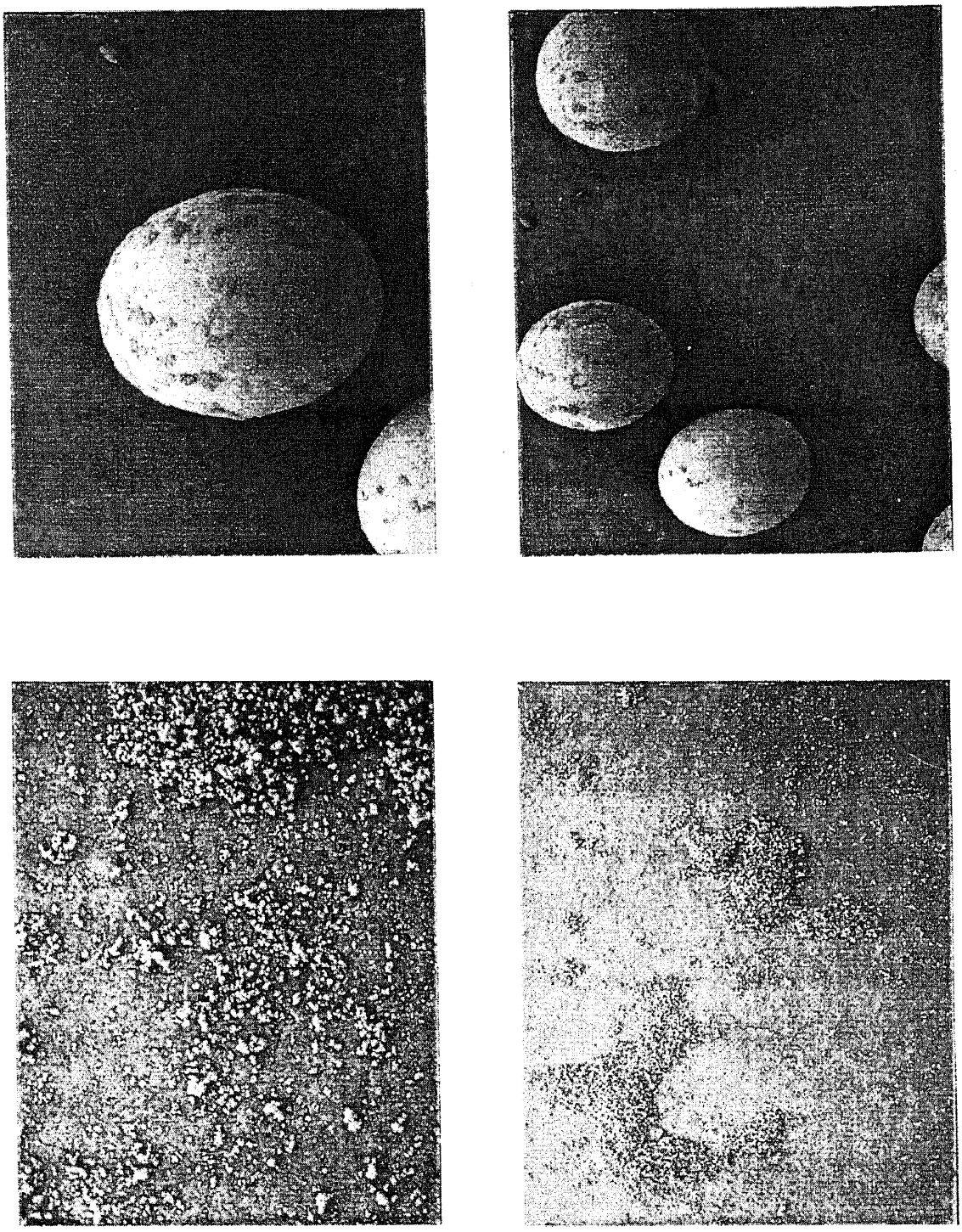

**Figure 2.7** SEM photograph of DCSMM process for 30 seconds, Alumina = 1g, Glass beads = 5g. **Observation:** Surface coverage is good, however there is formation of agglomerates of alumina.

## 2.3 Powder De-aggregation

In order to overcome agglomeration of guest particles and to achieve good surface coverage with host particles during dry coating, guest particles must have large surface area. Large surface area of guest particles can be achieved by breaking them into either smaller aggregates or singlets (individual particles).

Effective powder de-aggregation should overcome the forces of cohesion between the guest particles. Cohesive forces such as van der Waals force, moisture bonding forces, electrostatic force, solid bridging, and mechanical interlocking promote agglomerate formation of solid particles. If guest agglomerates are subjected to external forces or fields (shear, gravity, centrifugal force, etc.) greater than their inter-particle cohesive force, they will be broken up into their primary constituent particles. Usually, powders with particles exceeding 100μm in diameter show cohesion-less behavior; also, some powders with monodisperse size exhibit this behavior down to 30μm. As a general rule, a decrease in the contact area between particles results in lower cohesion, and hence particle shape and particle surface texture play an important role in determining the cohesive behavior of powders [15].

The Methods of de-aggregating powders may be classified based on the mechanism [16] involved, namely:

1. de-aggregation by acceleration flow or shear flow,
2. de-aggregation by impacting aggregates onto a solid target,
3. de-aggregation by mechanical force (fluidization, vibration, scraping,etc.), and
4. de-aggregation by depressurization, as described in the present work.

In present research, the guest powder is de-aggregated by the depressurization method developed at NJIT [17]. This is carried out by depressurizing a vessel filled with an aerosol of guest particles, through a short nozzle designed to minimize the role of shear forces. In this process, a known quantity of guest particles is placed inside a vessel followed by pressurizing with a gas. The act pressurizing the vessel generates the guest particle aerosol. This aerosol is then de-pressurized to ambient pressure through a short nozzle of known diameter resulting in disaggregation.

When the aggregates are porous, they become filled with compressed gas during pressurization and generation of aerosol. Thus, the gas pressure inside the aggregate is same as that inside the pressure vessel. During the discharge of aerosol from the pressure vessel through the nozzle, the pressure on and around the surface of the aggregate decreases rapidly decreases. As a result, the pressure difference between the inside of the aggregate and its surface increases. When this pressure difference is high enough, the forces generated by the escaping gas through the aggregate effects the break up of the guest powder into smaller aggregates or primary particles.

The mechanism of de-aggregation by depressurization is discriminated from that by shear flow or acceleration by considering the nature of fluid flow in a short nozzle, such as that used in our investigation. When the aerosol enters the capillary tube from the pressure vessel, there is a uniform velocity distribution at the entrance of the tube which transforms into a steady parabolic Poiseuille flow inside such tube. The length of the entrance section of the capillary tube in which uniform velocity distribution exists depends on the diameter of the tube and the Reynolds number of fluid flow [18], as given by equation 2.1

$$L_e = 0.1 d N_{Re} \tag{2.1}$$

where $N_{Re}$ is the Reynolds number, given by

$$N_{Re} = \frac{dV}{\nu} \tag{2.2}$$

where d is the diameter of the tube,

V is the velocity of fluid flow, and

$\nu$ is the kinematic viscosity.

Substituting appropriate values in the above equations, we found that the length of the entrance section of the pipe in which uniform velocity gradient exists exceeds the length of the orifice in our nozzle (which was approximately 1 mm). Thus, there is no velocity gradient occurring in the nozzle section and de-aggregation due to shear flow does not occur in our case. By using a smaller diameter nozzle, high vessel pressure and smaller quantity of guest particles we could achieve significant de-aggregation of powder [17].

## 2.4 Fluidization of Host Particles

In order to achieve uniformity of coating among host particles, it was proposed to coat them in fluidized state. Fluidization is the operation by which fine solids are transformed into a fluid-like state through contact with a gas or liquid. When a fluid flows upwards through a bed of fine particles, at low flow rates, fluid merely percolates through the void spaces between the stationary particles; this is called a "fixed" bed. At higher velocity, a

point is reached where the particles become suspended in the upward flowing gas or liquid. At this point, the frictional force between the particle and fluid counter balances the weight of the particle; the pressure drop through any section of the bed equals the weight of fluid and particles in that section. The bed is said to be "fluidized."

There are basically three techniques of coating in a fluidized bed, as shown in Figure 2.5:

1. top-spray using a conventional fluidized-bed granulator (Figure 2.5 (a));
2. bottom-spray using a Wurster-type column (Figure 2.5 (b)), or a spouted bed (Figure 2.5 (c));
3. tangential-spray using a rotor granulator (Figure 2.5 (d));

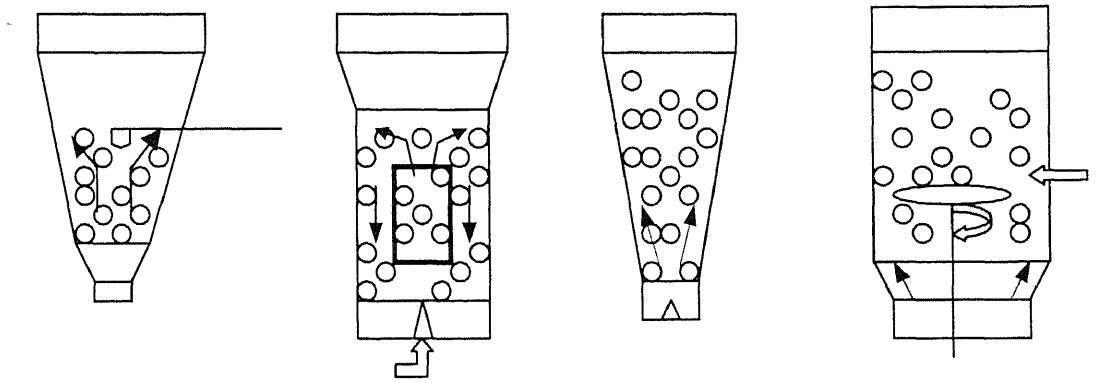


**Figure 2.8** Different configuration used in fluidized bed

Each system has its advantages and disadvantages. The bottom spray coating process produces relatively uniform coated particles [2]. The present study focuses on dry coating of particles in a spouted bed (DCPS) – i.e., the case show in Figure 2.5 (c).

In our investigation, a spouted bed is used where the aerosol fluid mixture flows upward through the center of the bed in the form of a column, causing a fountain-like

spout of solids at the top (Figure 2.5 (c)). The solids circulate downward around this fluid column. There are a number of variables that control the fluid dynamics in a spouted bed, namely:

1. Type of nozzle,
2. Location of nozzle,
3. Spray rate,
4. Atomization pressure,
5. Batch(host) size,
6. Velocity of fluidizing fluid,
7. Coating material (guest), and
8. Host particle properties.

## 2.5 Particle Collision in Spouted Bed

The nature of collision between guest and host particles in a fluidized bed is expected to determine the coating quality. Guest-host particle collision depends on the following factors: guest to host particle diameter ratios, guest to host mass ratio (concentration) and velocity of the fluid stream. Depending on the above factors there are two modes of collision : (a) large guest aggregate collision with host particles, and (b) small aggregate (or single particle) collision with host particles. In our case, large guest aggregates in the aerosol jet stream are produced when:

1. guest to host mass ratio is high,
2. aerosolizing pressure is low, and
3. nozzle diameter is large.

On the other hand, small aggregates (or singlet guest particles) are generated when:

1. guest to host mass ratio is low,

2. aerosolizing pressure is high, and

3. nozzle diameter is narrow.

In dry particle coating, the smaller the guest particle size (singlet or aggregate) and the smaller the difference in densities between the particle and medium, the weaker will be the inertial forces acting on such guest particles. In this case the guest particle trajectory will follow the host surface (without collision) resulting in poor coating. If the guest particle or aggregate size is larger, their forces of inertia are large enough to make them move in linear trajectories with respect to host particles thereby colliding with and coating the host surface. Therefore, an optimal guest particle size (with sufficient large surface area) and inertial force are needed to satisfy the conditions for a linear particle trajectory.

## 2.6 Dry Coating of Particles in Spouted Bed (DCPS)

The dry coating of particles in a spouted bed (DCPS) presently investigated in our research is a novel process for dry coating of particles. Glass beads, 500 microns, and submicron-to-micron size alumina and silica particles were used as host and guest, respectively. The glass beads were coated in a powder jet stream produced by the de-pressurization of a pressure vessel filled with guest powder aerosol. The coating takes place totally under dry condition without the use of solvents or binders.

In the DCPS process, coating involves three qualitative stages, as follows:

1. de-aggregation and aerosol production of guest particles,

2. transport of guest particles onto the surface of host particle, and

3. bonding (adhesion) of guest particles to the surface of host particles.

In this coating process, the aerosol of guest particles is rapidly depressurized into a bed of host particles. This rapid depressurization effects the de-aggregation of guest powder. The fluidization of host particles is caused by the kinetic energy of the fluid stream. During this process, the guest particles impact the host particle surface at a high velocity and coat them. The unique feature of this method is simplicity and potential use in industrial applications. This research provides a general understanding of the DCPS process, its feasibility, and its performance compared to dry coating by conventional mixing methods. In principle, a uniform coating can be achieved provided the host particles are well fluidized and every host particle receives the same flux of de-aggregated guest particles.

## 2.7 Coating Quality

The Coating quality refers to guest particle distribution and morphology on host particles. The methods used to examine coating quality in our work included:

1. Scanning Electron Microscopy (SEM),

2. Optical Microscopy, and

3. Quantification of coating efficiency by the "dissolution" test – Section 4.4.1

The first two methods gives qualitative information about the coating morphology, while the "dissolution" test gives quantitative information about the coating efficiency. In the present investigation, the "Coating Efficiency" is defined as the total weight of guest that adheres to host's surface per total weight of guest – see Section 5.1.

## 2.8 Conclusion to Chapter 2

1. Experimental investigation of dry coating by simple mechanical mixing revealed drawbacks such as non-uniformity among coated particles, poor de-aggregation and agglomeration of guest particles by compaction forces during this mixing process.
2. A novel dry coating technique based on coating of particles in a fluidized (spouted) bed is proposed. Preliminary results indicate that this process can overcome the drawbacks of coating by simple mixing processes.
3. Literature survey revealed that there is almost no coverage about dry coating by particles in aerosol stream. The closest is the work by Hiroyuki-Kage et al. [12] which was devoted to dry coating of particles in fluidized bed, but in the presence of wet binder spray.

# CHAPTER 3

# AEROSOL MECHANICS AND PARTICLE COLLISION – APPLICATION TO DRY COATING

The fundamental processes occurring during dry coating in a spouted bed relate essentially to the inertial deposition of guest particles from aerosol stream onto the surface of the host particles. Therefore, the coating rate of guest particles onto the host surface is expected to be a function of number of collisions (Section 3.2). The number of collisions is determined by the inertial fluid dynamic interaction of guest and host particles [18] (Section 3.1). To understand guest-host particle fluid dynamic interaction, an insight into aerosol mechanics is necessary. Application of Aerosol Mechanics to dry coating is a novel approach that is being explored in this thesis. Host particle behavior in fluidized bed, their sedimentation and fluidization fluid dynamics are discussed in Sections 3.3 and 3.4, respectively.

## 3.1 Host-Guest Inertial Fluid Dynamic Particle Interaction

Consider a collision of guest particles with the surface of host during the process of coating. As the aerosol flows around the host particles, guest particles may follow one of two trajectories, as shown in the Figure 3.1. If the guest particles are small and if the difference in density between guest and the fluid medium is small, weaker inertial forces will dominate and the particle trajectory follows the gas streamlines (line 2); thus they will "not" collide with the host particles (Figure 3.1A). This change in the course of the small-sized guest particle trajectory is caused by the long range fluid dynamic interaction; this occurs roughly at a distance equal to the host particle radius, away from the host

surface. In contrast, if the guest particle size is large, its trajectory is straight due to the forces of inertia and the probability of collision with the host particles is higher (line1). When the target distance, b < ( R + a) where 'R' is the radius of the host particle and 'a' is the radius of the guest particle, the guest particles moves linearly until it collides with the host particle surface (Figure 3.1A).

The host particle causes the flowing fluid to streamline around its surface and thereby streamlines the trajectory of small particles. This trajectory is called "grazing trajectory", Fig. 3.1 (B). In the case of large guest particles, the inertial forces exceed the long-range hydrodynamic interaction (LRHI) and hence their trajectories are not affected.

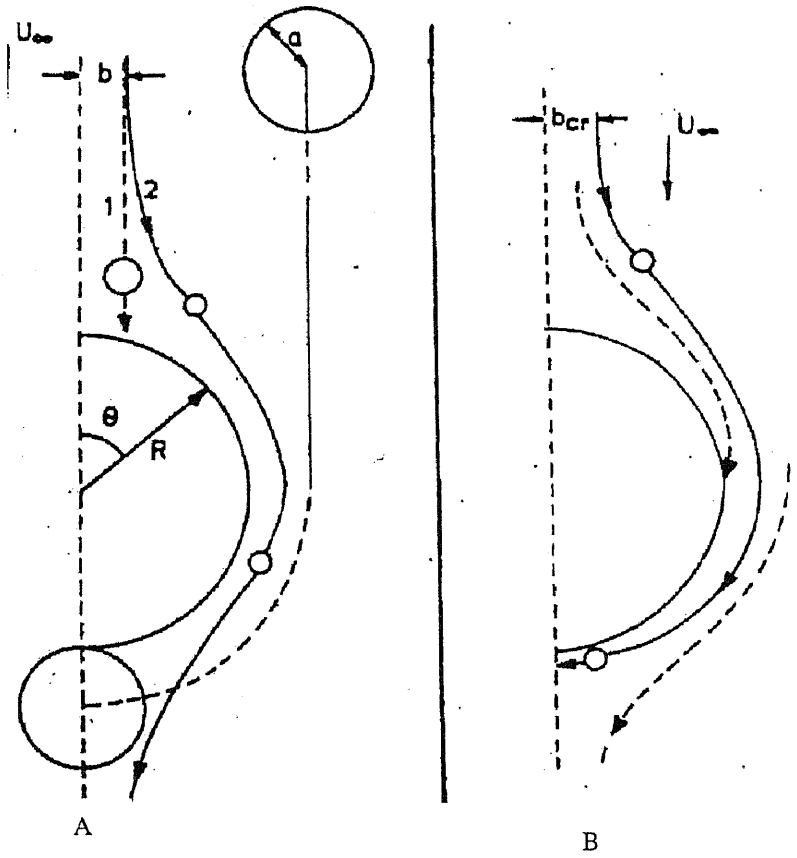


**Figure 3.1** Guest particle trajectory around a host particle **(A)** Influence of guest particle inertia on its trajectory in the vicinity of a host particle. Line 1 is the trajectory of a large particle and line 2 is the trajectory of a small particle at the same target distance, b. **(B)** Continuous line is the grazing trajectory of particles, dashed line is the trajectory of a

As a result, there is a critical guest radius below which collision with the host does not take place due to inertial forces. Otherwise, collisions can take place due to interception of guest particle trajectory by the host particles [19].

### 3.1.1 Determination of the Critical Guest Particle Radius for Collision with Host Particles

The distance the guest particle is able to pass through a viscous resistance of the fluid at an initial velocity of $U_\infty$ is given by [19]

$$L = \frac{2 U_\infty a^2 \rho_g}{9\nu} \tag{3.1}$$

where $\rho_g$ is the density of guest particle, $\nu$ is the kinematic viscosity of gas stream, and a is the radius of the guest particle. Since the host particle is impermeable to fluid, the normal component of the fluid velocity on its surface is zero. As distance from the host surface increases, the normal component of the fluid velocity also increases. The radius of fluid stream pipe, b approaching the host particle, in which the normal component of the fluid velocity decreases due to the effect of the host, is of the order of the host particle radius. The Inertial deposition of a guest particle on the host surface depends on the dimensionless Stokes parameter, as expressed by Equation 3.2.

$$St = \frac{2 \rho_g a^2 U}{9R\nu} \tag{3.2}$$

where $\rho_g$ is the density of the fluid stream, R is the radius of the host particle, a is the radius of the guest particle, and U is the velocity of the fluid stream approaching a host particle.

When St > 1, inertial deposition is possible, yet calculations have shown that it can also occur at St < 1 as long as St is not too small. This conclusion becomes apparent if a stream-pipe of aerosol of radius, R is considered and the guest particles in this stream-pipe approach the host surface not only due to inertial forces but also due to the motion of the fluid. The motion component of the guest normal to the host surface becomes zero at the surface of the host. Inertial deposition of the guest is impossible if St is smaller than critical Stokes parameter, $St_{cr}$, given by the following equation

$$St_{cr} = \frac{1}{12} = \frac{2\rho_g U a_{cr}^2}{9Rv} \tag{3.3}$$

where $a_{cr}$ is critical guest particle radius below which collision due to inertia does not occur.

When the Reynolds number is much greater than 80, the flow of the fluid around the host is a potential flow and when particle size is negligible, Levin found (1961) that inertial collision of guest particles with the host occurs if $a > a_{cr}$. If the size of guest particles is much greater than $a_{cr}$, the efficiency of coating increases, and thus the number of collision increases by increasing the size of the guest particles.

Collision Efficiency, a dimensionless parameter ε [19], is given by

$$\varepsilon = \frac{b_{cr}^2}{R^2} \tag{3.4}$$

where $b_{cr}$ is the maximum radius of the fluid stream pipe approaching the host such that all the guest particles in the stream pipe gets deposited on the host's surface [Fig.3.1]. Those guest particles that are not in the stream pipe are carried away by the fluid flow.

Langmuir derived [18] Equation 3.5 to describe the collision efficiency for inertial deposition of a smaller spherical particle onto the surface of a larger spherical particle. Fonda & Herne (1966) confirmed this equation is accurate in ±10%. The following relation was experimentally verified by Samygin et al. (1977) for Stokes number between 0.07 and 3.5 which gives the efficiency of guest particle collision with the host particle surface.

$$\varepsilon = \frac{St^2}{(St+0.2)^2} \tag{3.5}$$

where ε is collision efficiency, and St is stokes number.

In the potential flow regime, Collision Efficiency is given by equation 3.6

$$\varepsilon_p = \frac{3a}{R} \tag{3.6}$$

where $\varepsilon_p$ represents Collision Efficiency in potential flow regime around the host.

In Stokes regime, the equation for Collision Efficiency due to guest particle trajectory interception by host particles, derived by Derjaguin & Dukhin (1959) [19] is given by equation 3.7.

$$\varepsilon = \frac{3a^2}{2R^2} \tag{3.7}$$

The alumina particles and glass beads used in our work are almost spherical and the difference in their size is large. The collision efficiency of alumina particles with glass beads during coating in spouted bed was evaluated by Langmuir equation 3.5.

To vary the particle size, we rely on the size of aggregates generated in the coating experiments. Small aggregates have density approximately equal to the density of

alumina particles. However, larger alumina aggregates, which are more porous than smaller aggregates, have density between bulk powder density and single particle density. The powder density was found to be around 1.1g/cc. Stokes number and collision efficiency for various guest particle diameters, velocities and densities are evaluated and tabulated in Tables 3.1 and 3.2. Table 3.1 tabulates the results to particle density of 3.26g/cc, and Table 3.2 provides the results for the case of powder density of 1.16g/cc. The calculations involved in generating table 3.1 and 3.2 are in Appendix A

**Table 3.1** Stokes number and collision efficiency for various velocities and guest particle size (density = 3.26g/cc)

| V cm/s | 20 | | 50 | | 100 | | 200 | | 446 | | 1000 | | 2000 | | 5000 | |
|---|---|---|---|---|---|---|---|---|---|---|---|---|---|---|---|---|
| $r_g$ μ | St | ε | St | ε | St | ε | St | ε | St | ε | St | ε | St | ε | St | ε |
| 0.3 | 0.003 | 0.002 | 0.01 | 0.002 | 0.02 | 0.00 | 0.03 | 0.02 | 0.07 | 0.06 | 0.15 | 0.19 | 0.31 | 0.38 | 0.77 | 0.63 |
| 0.6 | 0.01 | 0.002 | 0.03 | 0.02 | 0.06 | 0.06 | 0.12 | 0.15 | 0.27 | 0.33 | 0.61 | 0.57 | 1.23 | 0.74 | 3.07 | 0.88 |
| 1.0 | 0.03 | 0.02 | 0.09 | 0.10 | 0.17 | 0.21 | 0.34 | 0.40 | 0.76 | 0.63 | 1.71 | 0.80 | 3.41 | 0.89 | | |
| 2.0 | 0.14 | 0.17 | 0.34 | 0.40 | 0.68 | 0.60 | 1.36 | 0.76 | 3.04 | 0.88 | 6.82 | 0.94 | 13.64 | 0.97 | | |
| 3.0 | 0.31 | 0.37 | 0.77 | 0.63 | 1.53 | 0.78 | 3.07 | 0.88 | 6.84 | 0.99 | 15.34 | 0.97 | 30.69 | 0.98 | | |
| 4.0 | 0.55 | 0.54 | 1.36 | 0.76 | 2.73 | 0.87 | 5.46 | 0.93 | 12.16 | 0.97 | 27.28 | 0.98 | 54.56 | 0.99 | | |
| 6.0 | 1.23 | 0.74 | 3.06 | 0.88 | 6.13 | 0.94 | | | | | | | | | | |

**Table 3.2** Stokes number and Collision efficiency for various velocities and guest particle size (density = 1.16g/cc)

| V cm/s | 20 | | 50 | | 100 | | 200 | | 446 | | 1000 | | 2000 | | 5000 | |
|---|---|---|---|---|---|---|---|---|---|---|---|---|---|---|---|---|
| $r_g \mu$ | St | ε | St | ε | St | ε | St | ε | St | ε | St | ε | St | ε | St | ε |
| 0.3 | 0.001 | $2x10^{-5}$ | 0.002 | $1x10^{-4}$ | 0.01 | 0.002 | 0.01 | 0.00 | 0.02 | 0.01 | 0.05 | 0.04 | 0.11 | 0.12 | 0.26 | 0.32 |
| 0.6 | 0.004 | $4x10^{-4}$ | 0.01 | 0.002 | 0.02 | 0.01 | 0.04 | 0.03 | 0.09 | 0.10 | 0.21 | 0.26 | 0.42 | 0.46 | 1.05 | 0.71 |
| 1.0 | 0.01 | 0.002 | 0.03 | 0.02 | 0.06 | 0.05 | 0.18 | 0.14 | 0.26 | 0.32 | 0.58 | 0.56 | 1.17 | 0.73 | 2.92 | 0.88 |
| 2.0 | 0.05 | 0.04 | 0.12 | 0.14 | 0.23 | 0.29 | 0.47 | 0.49 | 1.04 | 0.70 | 2.34 | 0.85 | 4.67 | 0.92 | 11.68 | 0.97 |
| 4.0 | 0.19 | 0.24 | 0.47 | 0.49 | 0.93 | 0.68 | 1.87 | 0.82 | 4.17 | 0.91 | 9.34 | 0.96 | 18.68 | 0.98 | 46.70 | 0.99 |
| 6.0 | 0.42 | 0.46 | 1.05 | 0.71 | 2.10 | 0.83 | 4.20 | 0.91 | 9.37 | 0.96 | 21.02 | 0.98 | 42.03 | 0.99 | 105.08 | 0.99 |
| 8.0 | 0.75 | 0.62 | 1.87 | 0.82 | 3.74 | 0.90 | | | | | | | | | | |

From the above Tables, we find that the collision efficiency for alumina particles is rather small even at higher velocities and considerably higher for aggregates of size 2-8μm is higher. Therefore, the coating process using aggregates of alumina should yield higher coating efficiencies. The quantitative dependence of coating efficiency on collision efficiency was accomplished by the derivation, given in Section 3.2.

### 3.2 Derivation of Coating-Collision Efficiency Relationship

Coating Efficiency is defined as the ratio of mass of guest that coats the surface of host particles to the initial amount of guest particles used. Its given by the equation:

$$\eta = \frac{\Delta m}{M_g} \tag{3.8}$$

where $M_g$ is the total amount of guest particles used, $\Delta m$ is the amount of guest that has coated the host particles. $\Delta m$ can expressed as the product of total number of host particles, $N_h$, and mass of coating per every host particle,$m_h$.

$$\Delta m = N_h m_h \tag{3.9}$$

$m_h$ which depends on guest particle concentration in the gas stream, $m_g$, fluid stream velocity, U, coating time, t, cross sectional area of the host particle, $S_h$ and collision efficiency, ε.

$$m_h = S_h m_g U t \varepsilon \tag{3.10}$$

Substituting equation (3.10) in (3.9), we get

$$\Delta m = N_h (S_h m_g U t \varepsilon) \tag{3.11}$$

The concentration of guest particles in the aerosol stream is given by:

$$m_g = \frac{M_g}{V_{gas}} \tag{3.12}$$

where $M_g$ = total mass of guest used, and $V_{gas}$ = total volume of fluid at ambient conditions. $V_{gas}$ can be expressed as the product of velocity of the fluid, U, cross sectional area of fluid flow in the fluidized bed, S and total time during which the fluid flows through the fluidized bed, t, i.e.,

$$V_{gas} = UtS \tag{3.13}$$

$$m_g = \frac{M_g}{UtS} \tag{3.14}$$

Substituting equation (3.14) in (3.12) and the resultant equation in equation (3.10), we get

$$m_h = \frac{S_h M_g \varepsilon}{S} \tag{3.15}$$

Substituting equation 3.15 in equation 3.9, we get equation 3.16

$$\Delta m = N_h \left(\frac{S_h M_g \varepsilon}{S}\right) \tag{3.16}$$

where $N_h$ is the ratio of total mass of host particles taken to mass of individual host particle

$$N_h = \frac{M_h}{m_h} \tag{3.17}$$

$$N_h S_h = \frac{M_h}{m_h} S_h = \frac{M_h 4\Pi R_h^2}{\frac{4}{3}\Pi R_h^3 \rho_h} = \frac{3M_h}{R_h \rho_h} \tag{3.18}$$

$$\Delta m = \frac{3M_h M_g \varepsilon}{R\rho_h S} \tag{3.19}$$

Substituting (3.19) in (3.8), we get the relation between Coating Efficiency and Collision Efficiency, which is:

$$\eta = \frac{3M_h \varepsilon}{R\rho_h S} \tag{3.20}$$

### 3.3 Analysis of Host Particle Sedimentation

Powder losses can occur in the pressure vessel and in piping due to possibility of sedimentation. The host particles also sediment during the process of coating in the coating chamber (spouted bed) and it is necessary to discriminate between collective host particle sedimentation and isolated host particle sedimentation in the spouted bed. Apparently, it is well known that collective host particle sedimentation velocity is equal to minimum fluidization velocity. Isolated host particle sedimentation is an extreme case of collective host particle sedimentation as their volume fraction approaches zero. Hence it is necessary to discuss the fundamentals of sedimentation before describing the process of fluidization in the spouted bed and in Section 3.5, isolated host particle sedimentation velocity is compared with minimum fluidization velocity of host particles.

In dry particle coating of guest over host, there are two forces acting on the host, namely, the external force and the drag force. The resistance of the fluid to the motion of guest particles, called *"Total Drag" force*, $F_D$, is proportional to the radius of the host particle, R and velocity of the fluid around the host, V. The Drag force given by Stoke equation [20] is.

$$F_D = -6\mu\pi RV \tag{3.21}$$

where $\mu$ is the viscosity of the aerosol that fluidizes the host particles. The external force acting on a host particle under the action of gravity (Inertial force) is given by,

$$F_w = \frac{4\pi R^3 g(\rho_p - \rho_g)}{3} = \frac{4\pi R^3 g \rho_p}{3} \tag{3.22}$$

where g is the acceleration due to gravity, $\rho_p$ and $\rho_g$ are the densities of the host particle and the gas respectively. As $\rho_g$ is small compared to $\rho_p$, $\rho_g$ is neglected.

Reynolds number of the particle is given by equation 3.23

$$N_{Re} = \frac{2R\rho_g V_s}{\mu} = \frac{2R V_s}{\nu} \tag{3.23}$$

where $\nu$ is kinematic viscosity, $V_s$ is rate of settling of particles

When Reynolds number is low, steady rate of settling of particles is given by equation 3.24

$$V_s = \frac{2R^2 g \rho_h}{9\mu} = g\tau \tag{3.24}$$

where $\tau = 2R^2\rho_h / 9\mu$, a quantity with the dimension of time, which plays an important role in the mechanics of aerosols. It is found that the error in Stokes law is approximately proportional to Reynolds number and is about 1.7% at $N_{Re} = 0.1$ and exceeds 5% at $N_{Re} = 0.5$.

As the radius of the host particle, the density of the particle and velocity of the fluid increases, the inertial and drag force on the particle also increases. In the region of higher Reynolds number, inertial forces cannot be neglected. Resistance of the medium to the motion of particles depends on two variables, namely, size and velocity of the particle. By using dynamic similarity, drag co-efficient, $\psi$ of a sphere (a dimensionless quantity) is expressed as unique function of Reynold's number [20], as expressed in equation 3.25

$$\Psi = \frac{2F_D}{\rho_g V^2 \pi R^2} \tag{3.25}$$

A number of empirical equations relating $\psi$ and Re have been proposed but the one proposed by Klyachko is simple and accurate [20] given by equation 3.26

$$\Psi = \frac{N_{Re}}{24} + \frac{4}{\sqrt[3]{N_{Re}}} \tag{3.26}$$

The above equation agrees well within 2% of $\psi$ values when Reynolds number varies between 3 and 400. Replacing for $F_D$ from equation 3.23 in equation 3.27, we get

$$N_{Re}^2 \Psi = \frac{8F_D\rho_g}{\pi\mu^2} \tag{3.27}$$

$$N_{Re}^2 \Psi = \frac{32 r^3 \rho_g \rho_g}{3\mu^2} \tag{3.28}$$

In order to find out the size of the particles from the rate of settling, the equation is

$$\frac{N_{Re}}{\Psi} = \frac{3 V_s^3 \rho_g^2}{4 \rho_g \rho} \tag{3.29}$$

The relation between particle size and settling velocity is given by Fuchs diagram, Figure 3.2. The falling velocity (sedimentation velocity) of an isolated host particle

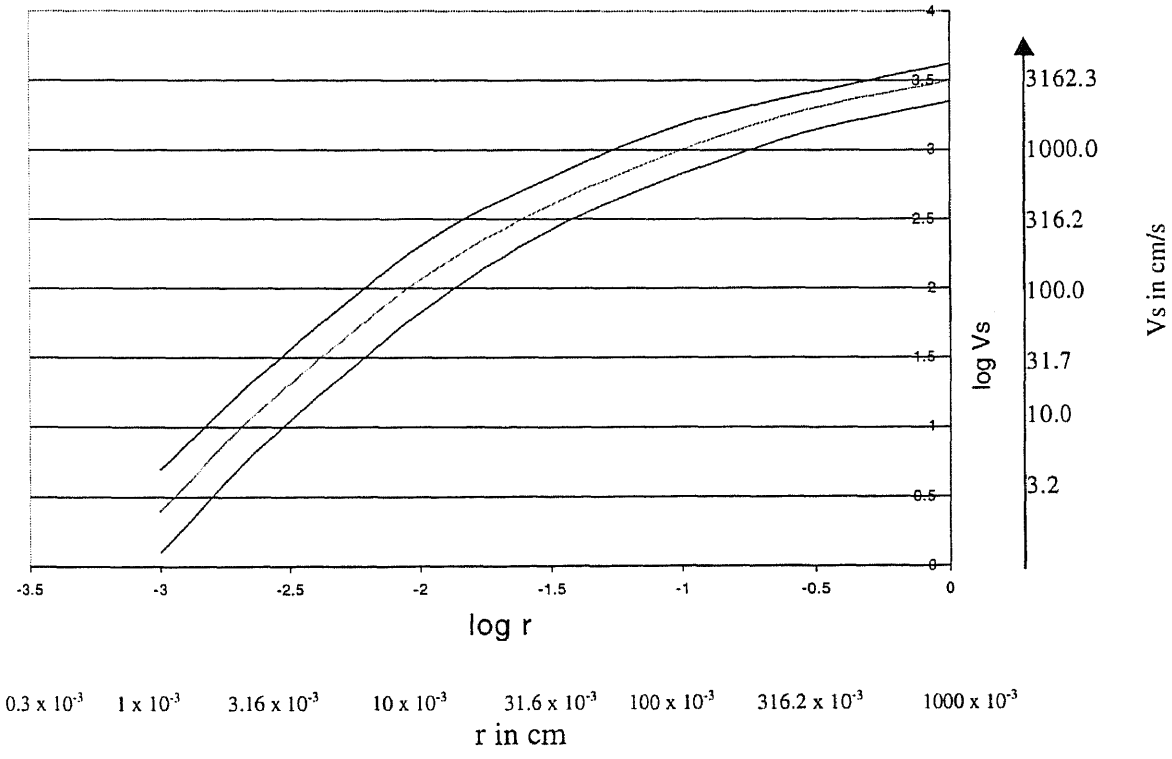


**Figure 3.2** Rate of settling of particles in air

(glass bead of density = 3.26g/cc, diameter = 500μm) during fluidization is found to be approximately 420cm/s.

### 3.5 Evaluation of Minimum Fluidization Velocity

For calculating the Stokes number and collision efficiency for guest-host particle collision in the spouted bed, the host particle velocity relative to guest particle velocity is necessary. The evaluation of this relative velocity is illustrated in Appendix F. This relative velocity should be greater than minimum fluidization velocity for self consistency of the experimental data acquired. Therefore, in this section fundamentals of minimum fluidization velocity and its evaluation for the experimental conditions are illustrated.

When a fluid is passed at very low velocity up through a bed of solid particles, the particles do not move. If the fluid velocity is steadily increased, the pressure drop and the drag on individual particles increase, and eventually the particles start to move and become suspended in the fluid. An equation for minimum fluidization velocity is obtained by setting the pressure drop across the bed equal to the weight of the bed per unit area of cross-section [21].

$$\Delta p.A_t = W = (A_t L_{mf})(1-\varepsilon_{mf})\left((\rho_s-\rho_g)\frac{g}{g_c}\right) \text{(reference 22)} \qquad (3.30)$$

where $\Delta p$ = pressure drop across the bed, $A_t$ is cross-sectional area of the tube, W is the weight of the bed per unit of the cross-section, $L_{mf}$ is the length of the bed at incipient fluidization, $\varepsilon_{mf}$ is the minimum porosity at incipient fluidization, $\rho_S$ is the density of solid host particles, $\rho_g$ is the density of gas.

By rearranging, we get

$$\frac{\Delta p}{L_{mf}} = (1-\varepsilon_{mf})(\rho_s - \rho_g)\frac{g}{g_c} \tag{3.31}$$

At onset of fluidization, the voidage is a little larger than that in packed bed and it corresponds to loosest state of packed bed of hardly any weight. The Ergun equation for pressure drop in packed beds is given by equation 3.33 [21].

$$\frac{\Delta p g_c}{L} = \frac{150\mu V_o (1-\varepsilon)^2}{\Phi_s^2 D_p^2 \varepsilon^3} + \frac{1.75\rho V_o^2 (1-\varepsilon)}{\varphi_s D_p \varepsilon^3} \tag{3.32}$$

Where $\phi$ is the sphericity for irregularly shaped particles is given by:

$$\varphi_s = \frac{6S_p}{D_p v_p} \tag{3.32a}$$

where $D_p$ is the diameter of host particles, L is the length of the packed bed of host particles, $\mu$ is the viscosity of aerosol stream, $S_p$ is the surface area of host particle, Vo is superficial velocity of aerosol stream in spouted bed and $v_p$ is the volume of host particle. Applying the above equation to the point of incipient fluidization gives a quadratic equation for minimum fluidization velocity, $V_{OM}$.

$$\frac{150\mu V_{om}(1-\varepsilon_M)}{\Phi_S^2 D_p^2 \varepsilon_M^3} + \frac{1.75\rho V_{om}^2}{\Phi_s D_p}\frac{1}{\varepsilon_M^3} = g(\rho_p - \rho_g) \tag{3.33}$$

For very small particles of small specific weight, the above equation simplifies to ($N_{Re,p} < 20$)

$$V_{om} = \frac{g(\rho_p - \rho_g)}{150\mu}\frac{\varepsilon_M^3}{(1-\varepsilon_M)}\Phi_s^2 D_p^2 \tag{3.34}$$

For large particles, minimum fluidization velocity ($N_{Rep} > 1000$) is given by

$$V_{om}^2 = \frac{\Phi_s D_p g(\rho_p - \rho_g)\varepsilon_M^3}{1.75\rho_g} \tag{3.35}$$

If $\varepsilon_m$ and or $\phi_s$ are unknown, the following modification of these expressions, suggested by Wen and Yu, can be used. First it was found for a wide variety of systems that [22]

$$\frac{1}{\Phi_s \varepsilon_M^3} \cong 14 \quad \text{and} \quad \frac{1-\varepsilon_M}{\Phi_s^2 \varepsilon_M^3} \cong 11 \tag{3.36}$$

Substituting the values in the equation for minimum fluidization velocity, gives Equation 3.45

$$\frac{D_p V_{om}\rho_g}{\mu} = \left[(33.7)^2 + 0.0408\frac{D_p^3 \rho_g(\rho_s - \rho_g)g}{\mu^2}\right]^{1/2} - 33.7 \tag{3.45}$$

Minimum fluidization velocity for small particles ($N_{Re,p} < 20$) is given by Equation 3.46

$$V_{om} = \frac{D_p^2(\rho_s - \rho_g)g}{1650\mu} \tag{3.46}$$

And for large particles ($N_{Re,p} > 1000$) [21,22]

$$V_{om}^2 = \frac{D_p(\rho_s - \rho_g)g}{24.5\rho_g} \tag{3.47}$$

Minimum fluidization velocity is evaluted for

Dp = Diameter of host glass beads = 500μm

$\rho_p$ = Density of glass beads = 3.26g/cc

g = 981 sq. cm / s .

The minimum fluidization velocity is found to be 32.30cm/s and is lesser than isolated host particle sedimentation velocity of 420cm/s (see Section 3.5). The experimental relative velocity between the guest and host particles should lie between the minimum fluidization velocity and isolated host particle sedimentation velocity. This is illustrated in Section in 5.2.2.

## 3.6 Conclusion to Chapter 3

1. Coating efficiency is directly proportional to collision efficiency. An equation is derived to calculate the coating efficiency from collision efficiency.

$$\eta = \frac{3 M_h \varepsilon}{R \rho_h S} \tag{3.20}$$

2. Collision efficiency and thus coating efficiency increases with increasing guest particle size and density.

3. Collision efficiency and thus coating efficiency is a function of guest particle velocity relative to host particle velocity.

4. For submicron particles, the collision efficiency is so small that coating efficiency is very low. It can be concluded that coating by sub-micron particles in aerosol stream is practically impossible. If the guest particles are aggregated (as in our case), the collision efficiency increases and thus resulting in high coating efficiencies.

# CHAPTER 4

# EXPERIMENTAL SET UP, PROCEDURES AND METHODS

## 4.1 Experimental Set Up

The experimental set up used in this research was designed such that the host particles were coated by guest powder jet aerosol in a fluidized bed. The powder jet was produced by the de-pressurization of a pressure vessel filled with the guest powder aerosol. This powder jet aerosol stream fluidized and coated the host particles in our experimental spouted bed .

A simple spouted bed coater was designed and constructed in our laboratory. Our set up consisted of a spouted bed and an aerosol spray generating system. Figure 4.1 is a schematic diagram of the entire system. The spouted bed (Figure 4.2) had a height of 60 centimeters. The bottom and top cross-sections were 1cm x 1cm and 3cm x 3cm, respectively. The spouted bed was built from wood and plexiglass (1/2" thickness), and was mounted on suitable supports. The wood was aligned at an angle of 5° to the vertical. The aerosol spray generating system consisted of a pressurized container (pressure vessel), an atomizing spray nozzle fitted located at the base of the spouted bed, two valves fitted to the pressure vessel, and a compressed carbon dioxide gas cylinder. The coating materials used were: glass beads (Potters Industries, Inc. PA, USA) host particles and Alumina (Sumitomo Chemical Co. Ltd, Japan) guest particles. The mean size of the glass beads and alumina particles were 500μm and 0.7μm, respectively. The host glass beads were chosen because they were almost spherical in shape. The as-received glass beads were colored with an organic coating that was found to affect the our results in

estimating the coating efficiency; this was attributed to the loss of this polymeric coating during the coating experiments. Prior to our experiments, we completely removed this polymeric coating by dissolving it in an organic solvent, followed by rinsing and drying the glass beads. The process of removing the organic coating from the as-received glass is described in Appendix B.

## 4.2 Experimental Procedure

A known quantity of guest powder and about five grams of host glass beads were placed in the pressure vessel and spouted bed, respectively. By opening the inlet valve, compressed carbon dioxide gas from the main cylinder was allowed into the vessel. The vessel was pressurized to the required pressure to produce preliminary aerosolization of guest particles inside said vessel. The outlet valve of the vessel was then opened to discharge and de-pressurize the compressed aerosol of guest powder through a nozzle of known length and diameter. The de-pressurization of the aerosol resulted in the de-aggregation of guest powder [18]. The de-aggregated powder jet stream effected the fluidization and coating of the glass beads in the spouted bed. At the end of the experiment, the coating chamber (spouted bed) was gently raised and the coated glass beads were collected in a clean container. Quantitative analysis of coating efficiency is discussed in Section 4.3.1, while the qualitative analysis of the coating produced is discussed in Section 4.3.2. The experiment was repeated to study the effect of different variables such as mass of guest particles, nozzle diameter, vessel size, pressure and other variables. The ranges of these variables are given in Table 4.1

**Table 4.1** Experimental variables

| | |
|---|---|
| Nozzle Diameter | 1000μm (1mm), 300μm (0.3mm) |
| Aerosolizing pressure in the vessel | 30psi, 40psi,50 psi, 140psi, 150psi, 300psi |
| Quantity of guest particles taken in the vessel | 0.1g, 0.15g, 0.3g, 0.7g, 1.0g, 1.5g. |
| Pressure vessel capacities | Large vessel = 2000cc (2 liters),<br>small vessel = 50cc (0.05 liters) |
| Guest particles (average size) | Alumina = 0.7μm |

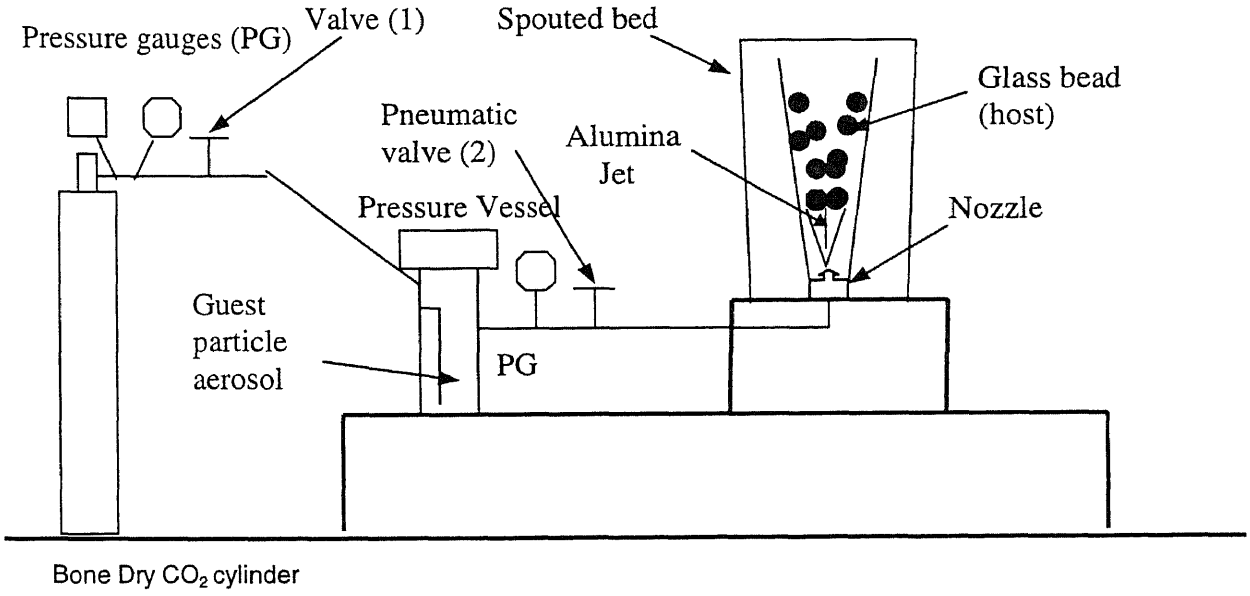


**Figure 4.1** Schematic diagram of dry coating of particles in spouted bed (DCPS)

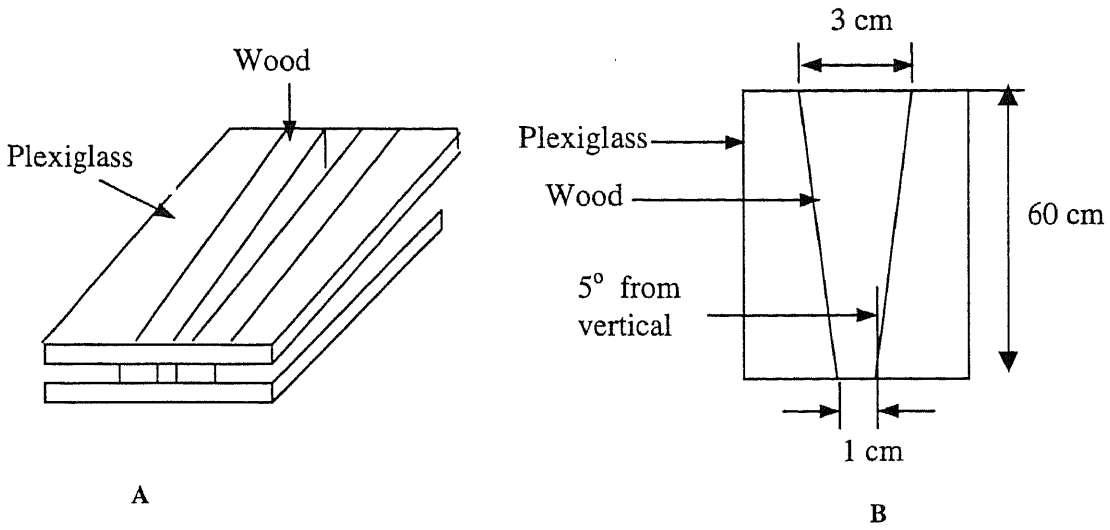


**Figure 4.2** (**A**) Schematic diagram of the spouted bed, (**B**) cross sectional view of spouted bed

## 4.3 Methods

### 4.3.1 Measurement of Mass of Coating on Host Particle Surface – Quantitative Analysis of Coating Efficiency

To estimate the amount of coating on the surface of the host particles, the following method was developed and used: The weight of an empty, clean and dry beaker, $m_1$ was determined. A sample of coated host was placed in the beaker and was weighed again ($m_2$). About 50cc of methanol was added to the beaker such that coated host particles were full covered by the liquid. The beaker was immersed in an ultrasonic bath and sonicated for 15 minutes. During ultrasonization, the guest particle coating are dislodged from the surface of the host particles and dispersed in methanol. Methanol along with dislodged alumina particles was decanted from the beaker. The process was repeated until all the coating is removed from the glass beads. The beaker containing clean host

particles was dried in an oven to a temperature of 150 C to drive away residual methanol and moisture. The mass of the beaker with de-coated host particles, $m_3$ , was obtained. The calculation of coating efficiency was done as follows:

Weight of sample of coated glass beads taken in the beaker = $m_2 - m_1$.

Weight of coating on sample of coated host = $m_3 - m_2$.

Coating efficiency, $\eta$ is defined as the ratio of total weight of guest that adheres to the host surface to the total weight of guest placed in the pressure vessel, is expressed as follows.

$$\eta = \frac{\text{Total wt. of coating on the host}}{\text{Total wt. of guest taken in the pressure vessel}} \tag{4.1}$$

$$\eta = \frac{m3 - m2}{m2 - m1} \times Mh \times \frac{1}{Mg} \times 100 \tag{4.2}$$

where $M_h$ is total weight of host particles taken (always 5grams), $M_g$ is total weight of guest particles taken.

### 4.3.2 Scanning Electron Microscopy and Optical Microscopy – Qualitative Analysis

The morphology of coating on the surface of host was studied using scanning electron (back scattering detector was used), and optical microscope. The results of qualitative morphology analysis are presented and discussed in Section 5.1.

# CHAPTER 5

# RESULTS AND DISCUSSIONS

In this Chapter, the results of dry coating in a spouted bed are presented and discussed in light of the aerosol mechanics relations developed in Chapter 3. A new method of evaluating coating quality is discussed in Section 5.2.2 and the coating results are compared with those obtained by powder mechanical mixing - Section 5.3.

## 5.1 Coating Results of Dry Coating of Particles in Spouted Bed

The results of dry coating of glass beads in an aerosol stream of alumina in a spouted bed can be divided into two main categories:

1. Coating with Large-Size Aggregated Alumina

   Mild de-aggregation of guest particles was achieved when aerosol of guest powder was de-aggregated at low pressures, using a wide diameter nozzle and by using small pressure vessel. Coating of glass beads with such large-size alumina aggregates yielded high coating efficiencies in the range of 30%-80% (Table 5.2, Figures 5.1 through 5.5).

2. Coating of Glass Beads with Small-Size Aggregated Alumina

   Good de-aggregation of guest powder was achieved when the aerosol of guest powder was de-aggregated at high pressures and coating by such small-size alumina aggregates yielded low coating efficiencies in the range of 5-20% (Table 5.2, Figure 5.4).

Several experiments were made to demonstrate the above two main results. The details of the experimental results are tabulated in appendix D.

### 5.1.1 Coating with Large-Size Aggregated Alumina

Large size guest aggregates were obtained when the aerosol of guest powder was generated under the following conditions: 30psi aerosolization pressure, 1mm nozzle diameter and 50 cc pressure vessel. The radius of the alumina aggregates generated by the above conditions was determined by aerosizer, and was found to be in the range of 9μm to 21μm – see Appendix C. Considering the aggregate size for the above conditions, both Stokes number and collision efficiency can be evaluated. From Equation 3.2, Stokes number is directly proportional to the square of the guest particle radius. Also, from Equation 3.5, collision efficiency, ε is proportional to the square of Stokes number. Simple calculations showed that collision efficiency was very close to one for the above conditions.

Therefore, when the size of the guest particle aggregates is large, the collision efficiency is high. From equation 3.20, the coating efficiency is directly proportional the collision efficiency and thus theoretically, the coating efficiency for such large aggregates is expected to be high. This was verified experimentally by achieving a high coating efficiency in the range of 30-85% (Table 5.1).

Under the above conditions, qualitative analysis of alumina coated glass beads by SEM and optical microscopy showed good surface coverage of 60-80% and, the relative variation of coating among coated host glass beads was low (Figures 5.1, through 5.5).

During the process of coating glass beads with large alumina aggregates, the kinetic energy of impact is dissipated by deforming such large aggregates at the surface of host particles leading to the formation of patches. The patches were observed under the optical microscope and were found to have a height to diameter ratio of 0.3-0.4. Coating thickness was determined theoretically (see Appendix H) and was found to be in agreement with the experimentally determined coating thickness (Table 5.2).

### 5.1.2 Coating with Small-Size Aggregated Alumina

Small aggregates of guest particles were obtained when the aerosol of guest powder was well aerosolized and de-aggregated at high pressures. From Appendix C, the mean size of guest aggregates under such conditions was in the range of 0.95μm to 2.1μm. From Equations 3.2, 3.5 and 3.20, the collision efficiency and thus coating efficiency are expected to be low. This was verified experimentally by carrying out coating of glass beads with alumina at high pressure of 150psi, where we achieved coating efficiency in the range of 5-20% (Table 5.1). Qualitative analysis by optical microscopy showed poor surface coverage of 15-25% and the relative variation of coating among coated glass beads was low.

Based on the analysis of coating under various conditions, the coating efficiencies for the large alumina aggregates were found to be higher than coating by well de-aggregated alumina powder (Table 5.2).

**Table 5.1** Summary of Coating Efficiency and Surface Coverage

| | Range of coating efficiency | Surface coverage* |
|---|---|---|
| Coating by large aggregates | 30 % - 85% | 60% - 80% |
| Coating by small aggregates | 5% - 20% | 15% - 25% |

* based on qualitative optical microscopic examination

**Table 5.2** Summary of Coating Results under different conditions

| | Sl. No. | Wt. of Alumina (g) | Nozzle diameter (mm) | Vessel Capacity (cc) | Operating Pressure (psi) | Size of aggregates –Aerosizer (μm) | Coating efficiency (%) |
|---|---|---|---|---|---|---|---|
| Coating with highly deaggregated alumina (Section 5.1.1) | 1 | 1.0 | 0.3 | 2000 | 150 | 2.116 | 4.9 |
| | 2 | 0.7 | 0.3 | 2000 | 150 | - | 9.5 |
| | 3 | 0.7 | 0.3 | 2000 | 150 | - | 13.2 |
| | 4 | 0.3 | 0.3 | 2000 | 150 | - | 17.1 |
| | 5 | 0.1 | 0.3 | 2000 | 150 | 0.9543 | 10.6 |
| | 7 | 1.0 | 1.0 | 2000 | 150 | - | 12.1 |
| | 8 | 0.7 | 1.0 | 2000 | 150 | - | 14.6 |
| | 9 | 0.3 | 1.0 | 2000 | 150 | - | 11.6 |
| | 10 | 0.15 | 1.0 | 2000 | 150 | - | 11.2 |
| | 11 | 0.7 | 1.0 | 50 | 150 | - | 14.3 |
| | 12 | 1.0 | 1.0 | 50 | 150 | - | 10.3 |
| Coated with aggregated alumina (Section 5.1.2) | 13 | 0.7 | 1.0 | 50 | 30 | 18.94 | 28.3 |
| | 14 | 1.0 | 1.0 | 50 | 30 | 24.26 | 84.8 |
| | 15 | 1.0 | 1.0 | 50 | 30 | 42.11 | 86.8 |
| | 16 | 0.7 | 1.0 | 50 | 30 | - | 72.2 |
| | 17 | 1.0 | 1.0 | 50 | 30 | - | 69.4 |

**Table 5.3** Comparison of theoretical and experimentally determined height of patches formed on surface of host during coating in spouted bed

| Average size of the alumina aggregates (aerosizer result) μm | Experimentally determined height of patch μ | Theoretically determined height of patch μ |
|---|---|---|
| 28 | 10 | 11 |

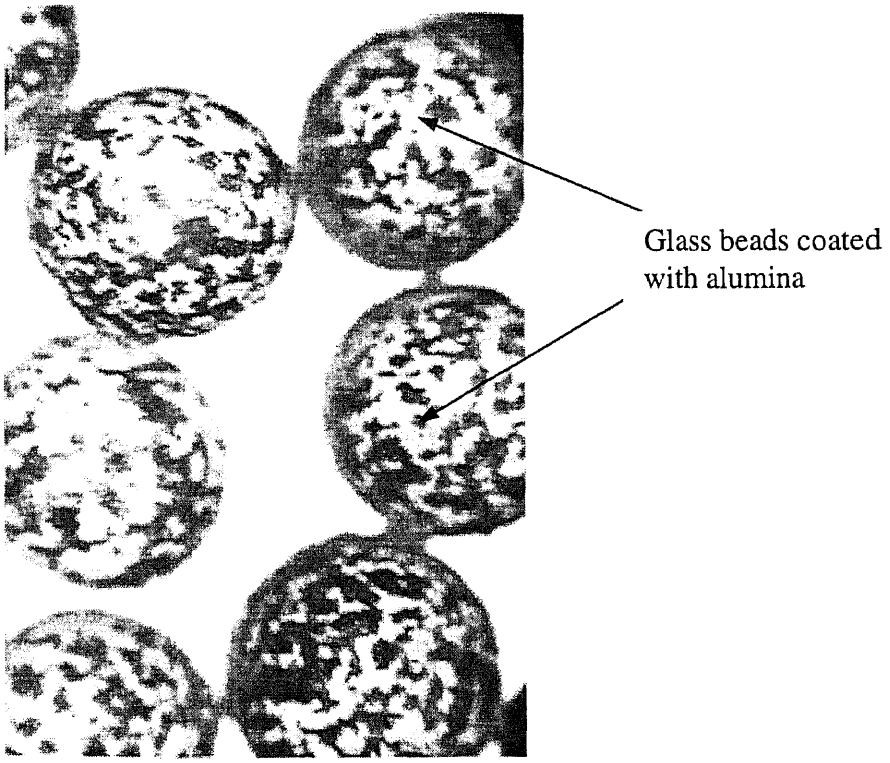


**Figure 5.1** Optical microphotograph of glass bead coated with large-size alumina aggregates, η=86.8%. Conditions: Nozzle diameter = 1mm, Alumina = 1 g, Glass beads = 5g, Pressure = 30 psi and Pressure Vessel Capacity = 50cc.**Observation:** The relative variation in coating of glass beads with alumina is very low, no residual alumina agglomerates.

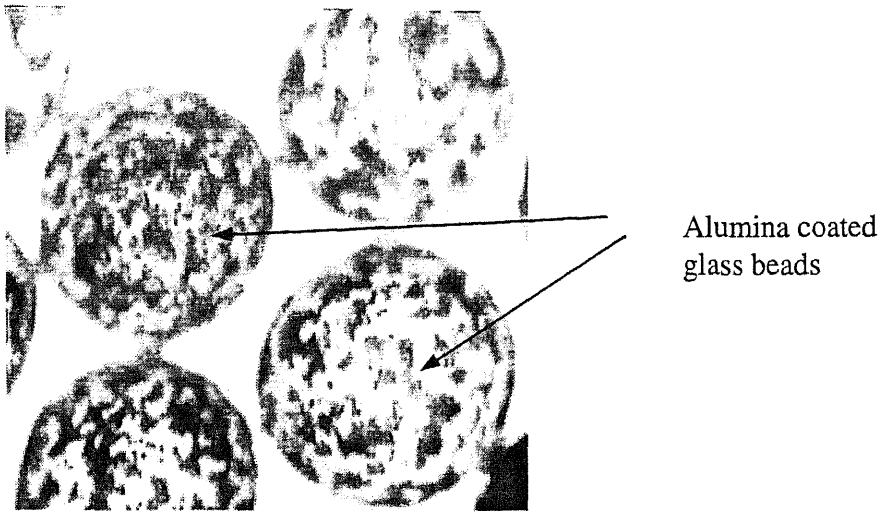


**Figure 5.2** Optical microphotograph of glass bead coated with large-size alumina aggregates, $\eta$ = 84.8%. Conditions: Nozzle diameter = 1mm, Alumina = 1g, Glass beads = 5g, Pressure = 30psi, Pressure vessel capacity = 50cc. **Observation**: Surface coverage is good and no aggregate formation of alumina particles

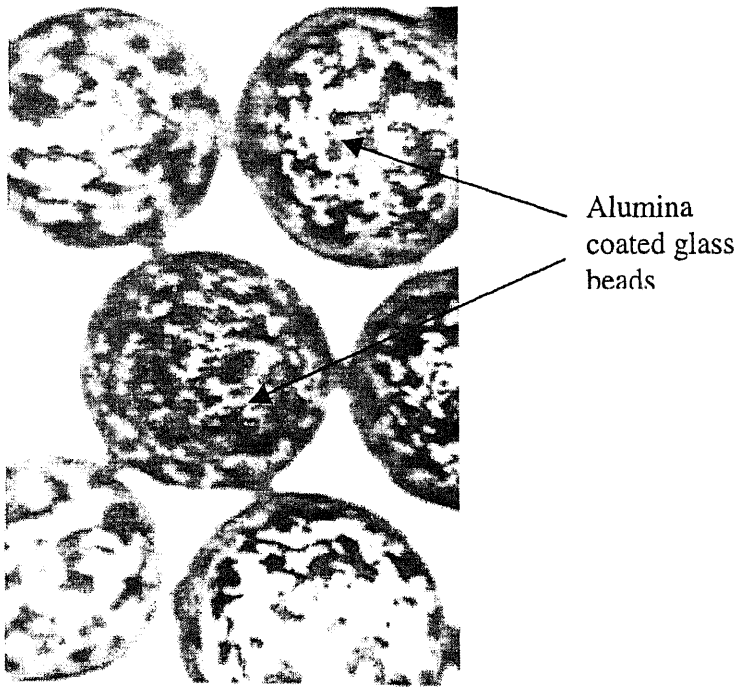


**Figure 5.3** Optical microphotograph of glass bead coated with large-size alumina aggregates, $\eta$=73.2%. Conditions: Nozzle diameter = 1mm, Alumina = 1g, Glass beads = 5g, Pressure = 30psi, Pressure vessel capacity = 50cc. **Observation:** Surface coverage is good and no aggregate formation of alumina particles

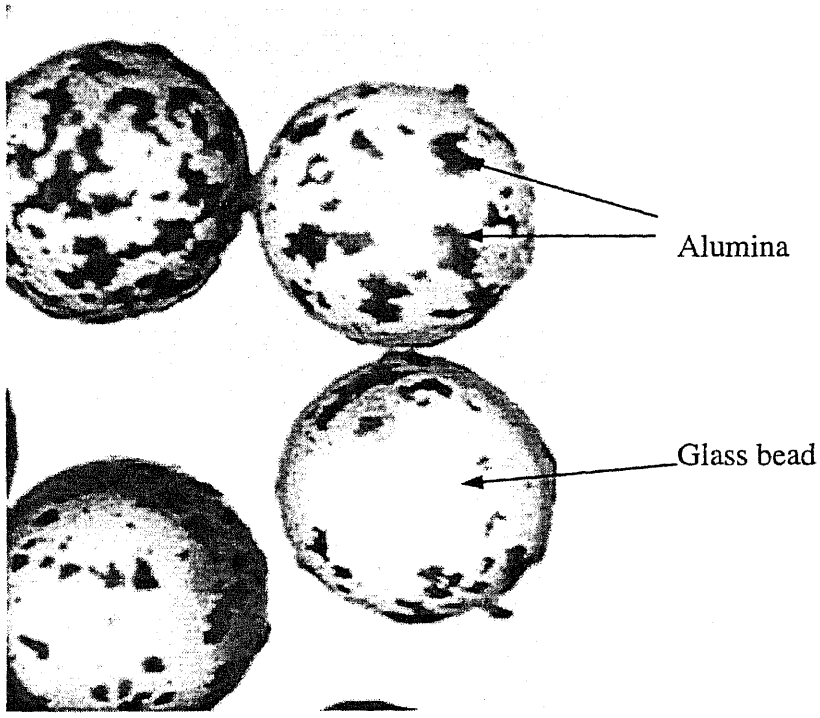


**Figure 5.4** Optical microphotograph of glass bead coated with small-size alumina aggregates, $\eta$= 4.9%. Conditions: Nozzle diameter = 0.3mm, Alumina = 1g, Glass beads = 5g, Pressure = 150psi, Pressure vessel capacity = 2000cc. **Observation:** Surface coverage by alumina particles on glass beads is poor and no agglomeration of

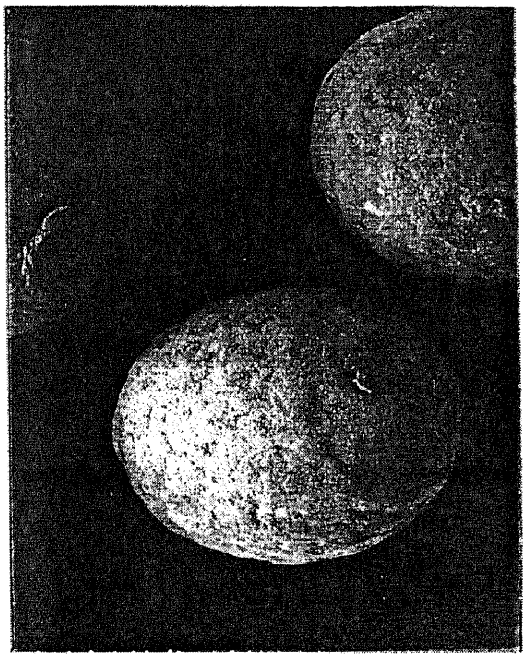

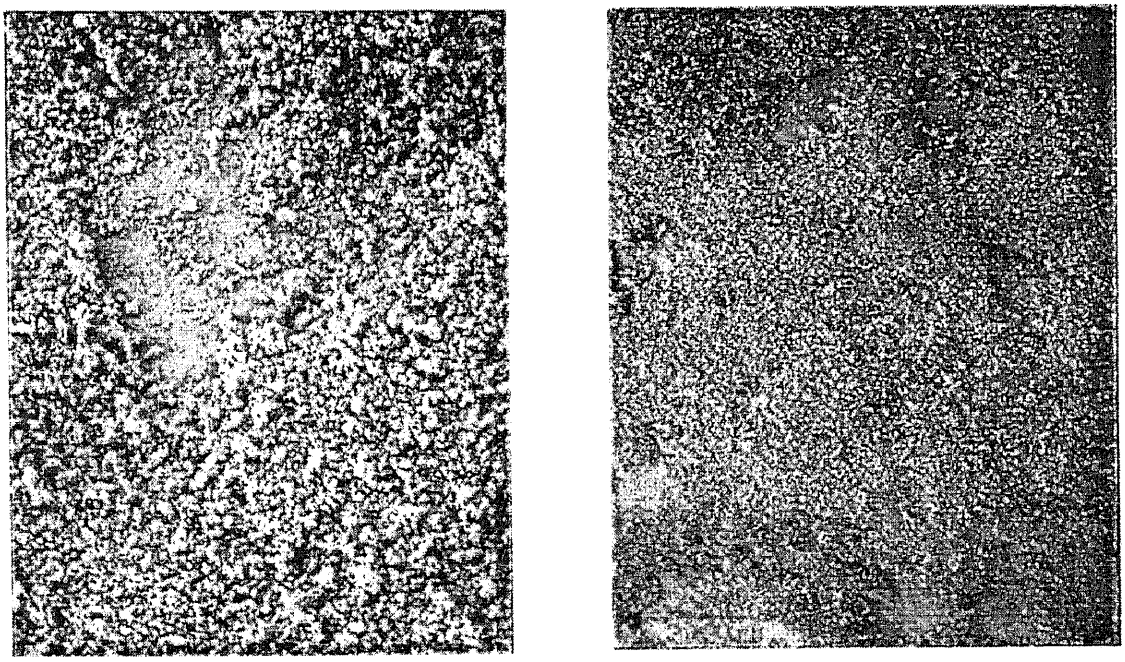

**Figure 5.5** SEM picture of glass bead coated with large-size alumina aggregates, $\eta$=86.8%. Conditions: SEM picture Nozzle diameter = 1mm, Alumina = 1g, Glass beads = 5g, Pressure = 30psi, Pressure vessel capacity = 50cc, Coating Efficiency = 86.8% **Observation:** Surface coverage is good and no aggregate formation of alumina particles

## 5.2 Interpretation of Results

### 5.2.1 Host Particle Trajectory during the Process of Coating

Host particle trajectory during the process of coating can be divided into three different paths, as shown in the Figure 5.11.

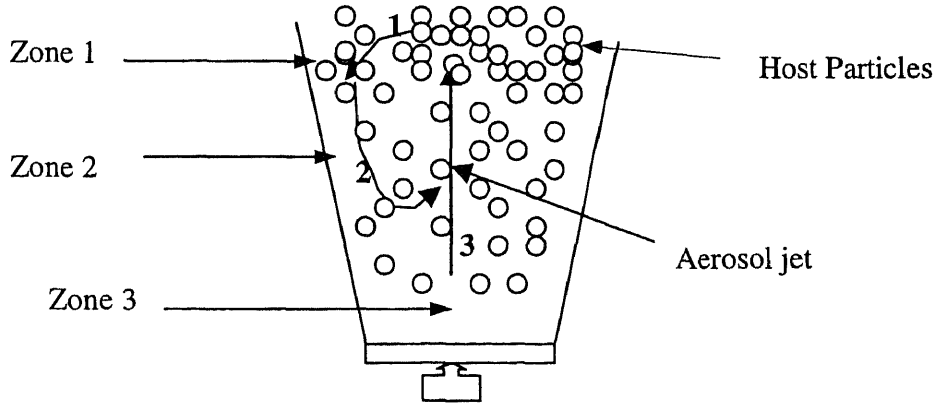


**Figure 5.6** Particle trajectory in spouted bed

During the process of fluidization, the velocity of host particles decreases with decrease in gas stream velocity and increase in fludization height. At a particular height of fluidization, the aerosol stream velocity equals the sedimentation velocity of the host particles, and the net velocity of host particles is zero in reference to the surroundings. The zone of the spouted bed where the net velocity of host particles is zero is termed "zone 1". At higher fluidization velocity, the particles cannot move further up as their sedimentation velocities exceed upward stream velocity and hence tend to move in radial direction. The particles begin to fall along the walls of the spouted bed (zone 2) and are

time of host particles in the region near to the nozzle (zone 3) is relatively much shorter than in zone 1. Therefore, we can assume that most of the coating occurs in zone 1 and th theoretical coating efficiency is calculated for this zone (see Section 5.2.2.).

Quantification of particle trajectory is not possible as there are no theories for gas trajectory restricted by walls of a spouted bed and jet turbulence suppression by particles.

### 5.2.2 Determination of Coating Efficiency from Collision Efficiency

From chapter 3, the relation between the coating efficiency and collision efficiency is as expressed by Equation 5.3 where

$$\eta = \frac{3 M_h \varepsilon}{R \rho_h S} \tag{5.1}$$

$M_h$ = mass of host particles placed in spouted bed = 5 grams,

R = radius of the host particle = 0.025 cm, and

$\rho_h$ = density of host particle = 2.26 g/cc.

From Section 5.2.1, we assume that cross-sectional area of zone one in the spouted bed (where most of the coating occurs) to be 2cm x 2cm. Substituting the above values in Equation 5.3, the relation between coating and collision is, as expressed by Equation 5.6

$$\eta = 66.37\varepsilon \tag{5.2}$$

The Collision efficiency, ε depends on the guest particle aggregate radius and the velocity of aerosol stream in the spouted bed. The velocity of the stream decreases with time and pressure in the vessel and the average velocity is found to be 50cm/s (Appendix F). This velocity is greater than minimum fluidization velocity of 32.30 cm/s (see Section 3.5) and

less than sedimentation velocity (420 cm/s) of isolated host particle in the spouted bed (see Section 3.3). This proves that our measured average velocity is consistent and is in the range of host particle sedimentation velocity and minimum fluidization velocity of the bed. The radius of guest particle aggregates is obtained from Aerosizer particle size analyzer (Appendix E). Collision efficiency for corresponding guest particle radius and velocity is evaluated from Table 3.2 and is substituted in Equation 5.6. The results of theoretically determined coating efficiency are tabulated in Table 5.4.

**Table 5.3** Determination of theoretical coating efficiency from collision efficiency

| Sl. NO. | Pressure (psi) | Pressure Vessel capacity (cc) | Nozzle diameter (mm) | Amount of guest (g) | Collision efficiency | Theoretical coating efficiency |
|---|---|---|---|---|---|---|
| 1 | 150 | 2000 | 0.3 | 0.1 | $2.2 \times 10^{-4}$ | 55.56% |
| 2 | 150 | 2000 | 0.3 | 1.0 | $30.14 \times 10^{-4}$ | 130.88% |

Table 5.3 demonstrates the range of theoretical coating efficiency for two extreme cases, namely 0.1 gram and 1.0 gram of guest particles. Theoretically determined coating efficiency for well de-aggregated particles at high pressures ranges from 55% to 130%. Experimentally determined coating efficiency for the same conditions of good de-aggregation lies in the range of 5% to 20%. The reason for the large difference in theoretical and experimental coating efficiency is attributed to powder losses as illustrated in Section 5.2.2.1.

**5.2.2.1 Underevaluation of Experimental Coating Efficiency caused by Powder Losses in Vessel and in Pipings:** In our experiment, the pressure vessel containing guest powder is pressurized with carbon dioxide to generate an aerosol of guest particles. The duration of this compressed aerosol release is long and varies from 30 seconds to 400 seconds for different experiments. During the process of aerosol release into the spouted bed, there is a possible sedimentation of guest particle aggregates to the bottom of the vessel or inside the pipes. Thus the powder is lost due to sedimentation and thus becomes unavailable for coating. The experimental coating efficiency achieved is low compared to theoretical coating efficiency due to possible powder losses in the vessel and pipe. In Equation 4.2,

$$\eta = \frac{m_3 - m_2}{m_2 - m_1} \times M_h \times \frac{1}{M_g} \times 100 \qquad (5.3)$$

appropriate value for $M_g$ should be substituted taking into account the powder losses.

When the radius of a guest particle aggregate is greater than a certain guest particle radius (Critical Guest Particle Radius (CGPR)), the aggregate or the particle may sediment to the bottom of the vessel or the pipe. Critical guest particle radius depends on aerosolization pressure and vessel capacity. Appendix G tabulates critical guest particle radius for various aerosolization pressures and vessel capacities.

## 5.3 Comparative Study of Dry Coating of Particles in Spouted Bed and Dry Coating by Simple Mechanical Mixing

In dry particle coating by simple mechanical mixing (DCMM), the aggregates of guest particles deformed and de-aggregated between the host particles and adhered to the surface of the host. However, the cohesion between the guest particles was stronger than

adhesion between the guest and host particles. This cohesion favored compaction over de-aggregation and deformation of guest particles, resulting in non-uniform poor coating of glass beads and agglomeration of guest particles.

In dry coating of particles in spouted bed (DCPS), the cohesion between guest particles was overcome by de-aggregation of aerosol of guest particles and this prevented agglomeration of guest particles. Moreover, the guest particle aerosol stream fluidized the host particles in the spouted bed, ensuring almost the same guest particle flux to each of the host particles during coating, resulting in little variation of coating among coated glass beads

## 5.4 Conclusions to Chapter 5

1. In DCPS proces, coating glass beads with large aggregates of alumina particles yielded a better surface coverage and high coating efficiencies than coating with smaller aggregates of alumina particles.
2. Theoretical coating efficiency was determined on the basis of aerosol mechanics relation developed in Chapter 3.
3. Experimentally determined coating efficiency is lower than theoretically determined coating efficiency due to guest particle losses in the vessel and in the piping during the DCPS process. A correction factor can be introduced taking into account these powder losses while determining experimental coating efficiency.
4. The relative variation of coating among coated host particles in DCPS method was very low compared to coating by simple mechanical mixing method.

5. The agglomeration of guest particles was overcome by the prior de-aggregation of guest particle aerosol in DCPS process and thus eliminating the drawbacks of coating by mechanical mixing method.

# CHAPTER 6

# CONCLUSIONS AND RECOMMENDATIONS FOR FUTURE RESEARCH

## 6.1 Conclusions

This thesis was been devoted to the study of a novel dry coating of particles method in fluidized bed. The main objectives of this work were to study the feasibility of the process, both quantatively and qualitatively, and to compare the results with coating by simple mechanical mixing. A separate section was dedicated to account for the collision between guest and host particles and to show how collision efficiency affects the coating efficiency. The main results of this work can be summarized as follows:

1. A rather high coating efficiency of 60-80% was achieved when aggregates of alumina particles were used to coat the glass beads in a spouted-fluidized bed.
2. It was found both experimentally and theoretically that collision efficiency and coating efficieny of large aggregates of guest particles onto surface of host particles was higher than that of small aggregates of guest particles.
3. An equation relating the coating efficiency and the collision efficiency was derived, and experimentally substantiated.
4. The relative variation of coating among coated host particles was much less by dry coating of particles in spouted bed (DCPS) process than dry coating by simple mechanical mixing(DCSMM). In DCPS process, it was observed that the surface coverage of coating improved by increasing the ratio of guest to host particles.
5. The high coating efficiency and good surface coverage achieved by DCPS process is attributed to flattening of large aggregated guest particles on the surface of host particles,

caused by high guest aggregates impact velocities. The characteristic feature of the patches formed on the host surface was, the ratio of diameter of height of the patch varied from 5 to 10.

6. The mechanism behind not achieving complete surface coverage of host during coating is proposed and quantified (see Section 6.2).A method for achieving better surface coverage can be achieved by separating the coating zone from the zone of high velocity of the guest aerosol jet can be made. This should prevent guest aggregate rebound and tangential removal in high speed fluid stream.

## 6.2 Recommendation for Future Research

During the process of de-pressurization of a vessel filled with guest powder aerosol, there is a zone of high velocity close to the nozzle exit in the coating chamber. In this zone, there is a possibility of tangential removal of coating from the coated host surface and guest particles may rebound from the host surface during coating. This phenomenon of particle rebound and tangentially removal can be curtailed by reducing the residence time of the host particles in the high velocity zone. This can be done by inserting a pyramid shaped solid block with a concentric cylindrical hole, as shown in Figure 6.1. During coating, the host particles are fluidized and most of them circulate above the solid block, thus reducing their residence time in the high velocity zone and increasing it's residence time in the coating zone. Test of this new fluidized bed design needs to be further developed in future investigation of the dry coating process.

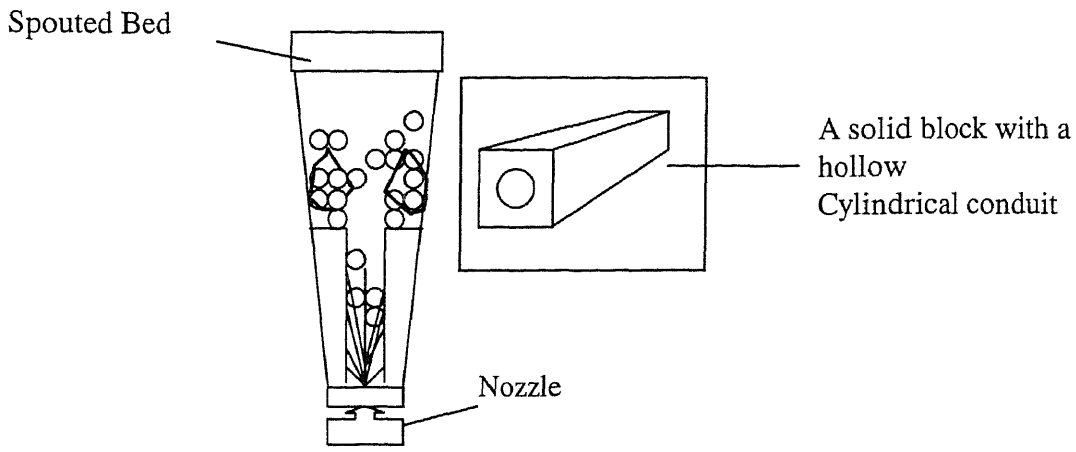


**Figure 6.1** Schematic diagram of a spouted bed fitted with a pyramid shaped solid block with concentric cylindrical hole

### 6.3 Optimum Guest Particle Size and Coating with Aggregates

In dry particle coating, if the guest particle size is very small, the coating is poor due to low collision efficiency (Section 3.2). Coating with large single particles would result in poor coating due to high probability of guest particle rebound from the surface of the host. Rebound of guest particle from host particle surface occurs due to their high kinetic energy of impaction [23]. Thus coating by singlets (single particles) is possible in a narrow range of guest particle size. Using an optimal aggregate dimension should produce both high coating efficiency and uniformity. Quantative investigation of this area is needed. This difficulty can be overcome by coating the host particles with aggregates. As the aggregates are heavier than singlets their collision efficiency is greater than that for singlets. Moreover, rebound of guest particle aggregates is reduced because the kinetic

energy of impaction results in flat patches on the host surface. This increases the number of points of contacts between guest particle aggregates and host surface which prevents rebound from the host surface. This phenomenon of aggregate adhesion and flattening at the host's surface has resulted in rather high coating efficiency in our experiments. Quantative analysis of rebound of large single particles and absence of rebound phenomenon for aggregates is a separate non-trivial task which is beyond the scope of this preliminary investigation.

### 6.4 Nature and Limitation of this Investigation

Dry coating of particles by aggregated aerosol in spouted bed can be considered as the first step in the investigation of a new phenomenon of dry coating. Many questions arise in the investigation of a new phenomenon and naturally only some of them was possible to be investigated in this work. The mechanism and its preliminary quantification are presented in this thesis but process is more complicated than the model adopted here, for example, there are 3 coating zones (Section 5.2.1) and coating is quantified for only one zone assuming that coating in other two zones are small. The reproducibility of the equipment was poor and there were coating losses in pipings and vessel. Thus this accomplished experiment can be characterized as semiquantitative and there is scope for improving the experimental conditions.

## APPENDIX A

## EVALUATION OF STOKES NUMBER AND COLLISION EFFICIENCY

Calculations involved in generating table 3.1 are, as below:

Stokes Number is given by

$$St = \frac{2 r_g^2 V \rho_g}{9Rv} \qquad (A.1)$$

Where $r_g$ = radius of the guest particle

V is the velocity in cm/s

$\rho_g$ is the density of the guest particle in g/cc = 3.26 g/cc

R is the radius of the host particle in cm = 0.025cm

v is the kinematic viscosity of the fluid = 1.7 x $10^{-4}$ $cm^2/s$

Considering Alumina singlet particle density (3.26 g/cc), we get stokes equation as

$$St = \frac{2 \times 3.26 \times r_g^2 \times V}{9 \times 0.025 \times 1.7 \times 10^{-4}} = 1.704 \times 10^{-3} \times r_g^2 \times V \qquad (A.2)$$

$r^2_g$ in sq.μm = $r^2_g$ 10-8 sq.cm

Collision Efficiency given by Langmuir Equation is

$$\varepsilon = \frac{St^2}{(St + 0.2)^2} \qquad (A.3)$$

Calculations involved for generating table 3.2 are as below

$\rho_g$ is the density of the guest particle in powder form = 1.1165 g/cc ...

$r_h$ is the radius of the glass beads (host particle) in cm = 0.025cm

$\nu$ is the kinematic viscosity of the fluid = $1.7 \times 10^{-4}$ $cm^2/s$

$$St = \frac{2 \times 1.12 \times r_g^2 \times V}{9 \times 0.025 \times 1.7 \times 10^{-4}} = 5.84 \times 10^{-4} \times r_g^2 \times V \qquad (A.4)$$

Considering Alumina powder density = 1.16 g/cc, we get stokes equation as

$r^2_g$ in sq.$\mu$m = $r^2_g$ 10-8 sq.cm

Collision Efficiency given by Langmuir Equation is calculated using equation A.3

## APPENDIX B

## PREPARATION OF HOST PARTICLES

The host particles were stripped off its pigmentation by using methanol and acetone. A known amount of colored host was taken a clean glass beaker and a required amount of methanol was added to it such that all the particles were completely rinsed in it. The beaker was placed in an ultrasonic bath and ultrasonized for about fifteen minutes. The host particles were partly decolorized and the pigment contaminated the methanol and by decanting the beaker, most of the methanol was drained out. The beaker was then placed in an oven and heated to a temperature of 150-170°C to remove traces of methanol. The weight of the beaker was found out. The host particles were stripped off its residual pigmentation by using acetone. Required amount of acetone was added to the beaker that contained partly decolorized host particles. It was ultrasonized, decanted, heated and weighed again. The process of acetone stripping was repeated until the difference in weight of beaker between consecutive stripping process was almost zero. The results were, as follows:

1. Weight of empty beaker = 147.34 g

2. Wt. of empty beaker + colored host = 372.84 g

3. Wt. of colored host taken = 225.5 g

*Methanol Wash*:

4. Wt. of empty beaker + partly decolorized host = 372.64 g

*Acetone Wash*:

4. Wt. of empty beaker + partly decolorized host = 372.50 g

4. Wt. of empty beaker + partly decolorized host = 372.50 g
5. Wt. of empty beaker + partly decolorized host = 372.43 g
6. Wt. of empty beaker + partly decolorized host = 372.39 g
7. Wt. of empty beaker + partly decolorize[d] 70 372.39 g
8. Wt. of empty beaker + partly decolorized host = 372.39 g
9. Wt. of empty beaker + decolorized host = 372.38 g
10. Wt. of empty beaker + decolorized host = 372.38 g

The completely decolorized host particles were used for the coating process in the spouted bed.

## APPENDIX C

## AEROSIZER PARTICLE SIZE ANALYSIS

In this appendix, the results of Particle size analysis evaluated by API Aerosizer instrument for various experimental conditions are, as follows:

*1) Experimental conditions*:

Nozzle diameter = 0.3mm

Aerosolization pressure = 150psi

Amount of guest particles taken in the vessel = 0.1 gram

Pressure vessel capacity = 2000cc

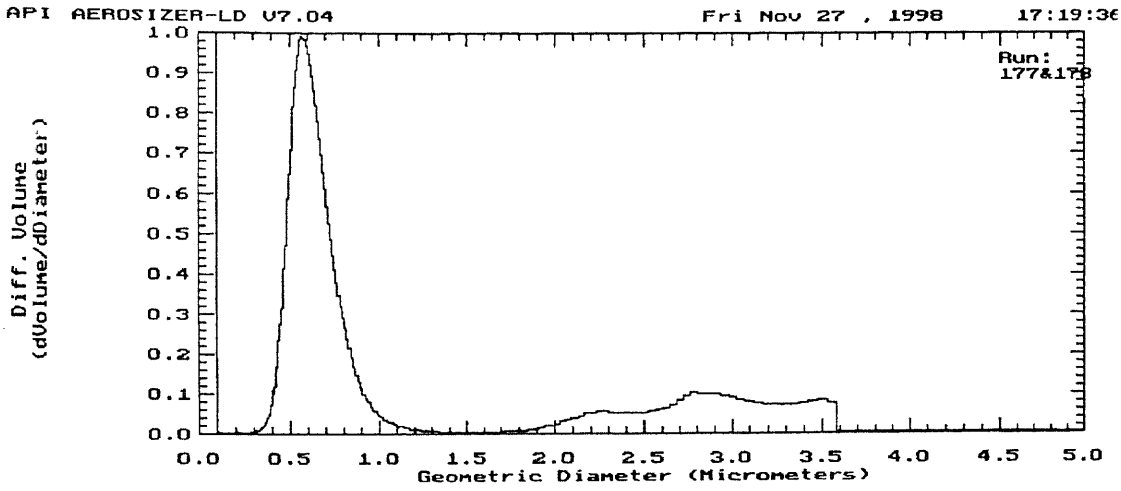


**Figure C1** Aerosizer volumetric particle size distribution for the following conditions: Nozzle diameter = 0.3mm, Pressure = 150psi, Guest =0.1g and Vessel 2000cc

***Mean size = 0.9543μm***

Disperser type = Pulse jet

Standard Deviation = 2.046

Mode (linear scale) = 0.56

Alumina density = 3.26 g/cc

Specific area = 2.36 sq. meter/g

Flow rate range = 1.88 l/min – 2.00 l/min

Concentration = 4.16 X $10^6$ particles / cubic meter (counting efficiency = 1.0)

Mass loading = 1.94 x $10^{-3}$ mg/ cubic meter (counting efficiency = 1.0)

| % under | %size | %under | %size |
|---|---|---|---|
| 5% | 0.4664 | 55% | 0.7111 |
| 10% | 0.4992 | 60% | 0.7554 |
| 15% | 0.5234 | 65% | 0.8219 |
| 20% | 0.5443 | 70% | 1.010 |
| 25% | 0.5642 | 75% | 2.259 |
| 30% | 0.5839 | 80% | 2.628 |
| 35% | 0.6042 | 85% | 2.844 |
| 40% | 0.6259 | 90% | 3.050 |
| 45% | 0.6499 | 95% | 3.320 |
| 50% | 0.6776 | | |

*2. Experimental conditions*

Nozzle diameter = 0.3mm

Aerosolization pressure = 150psi

Amount of alumina taken in the vessel = 1.0 grams

Pressure vessel capacity = 2000cc

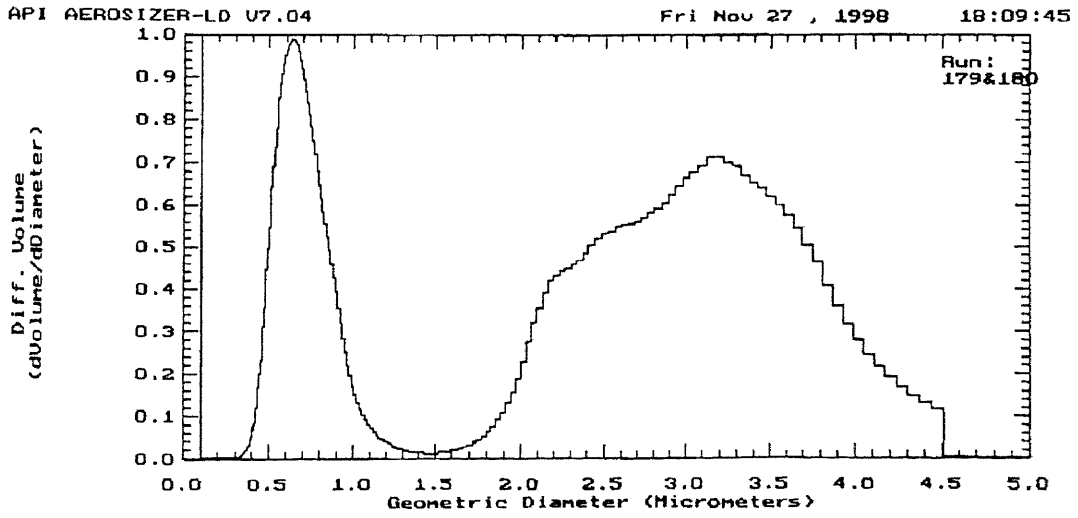


**Figure C2** Aerosizer volumetric particle size distribution for the following conditions: Nozzle diameter = 0.3mm, Pressure = 150psi, Guest = 1.0g, Vessel = 2000cc

***Mean size = 2.116μm*** Disperser type = Pulse jet

Standard Deviation = 1.951 Mode (linear scale) = 0.63

Alumina density = 3.26 g/cc Specific area = 1.13 sq. meter/g

Flow rate range = 1.88 l/min – 1.92 l/min

Concentration = 4.35 X $10^6$ particles / cubic meter (counting efficiency = 1.0)

Mass loading = 7.70 x $10^{-3}$ mg/ cubic meter (counting efficiency = 1.0)

| % under | %size | %under | %size |
|---|---|---|---|
| 5% | 0.5662 | 55% | 2.928 |
| 10% | 0.6478 | 60% | 3.048 |
| 15% | 0.7349 | 65% | 3.161 |
| 20% | 0.8604 | 70% | 3.272 |
| 25% | 1.890 | 75% | 3.389 |
| 30% | 2.185 | 80% | 3.514 |
| 35% | 2.36 | 85% | 3.649 |
| 40% | 2.515 | 90% | 3.808 |
| 45% | 2.659 | 95% | 4.041 |
| 50% | 2.798 | | |

*3. Experimental conditions*

Nozzle diameter =1mm,

Aerosolization pressure = 30psi,

Amount of alumina taken in the vessel = 1.0 grams, and

Pressure vessel capacity = 50cc

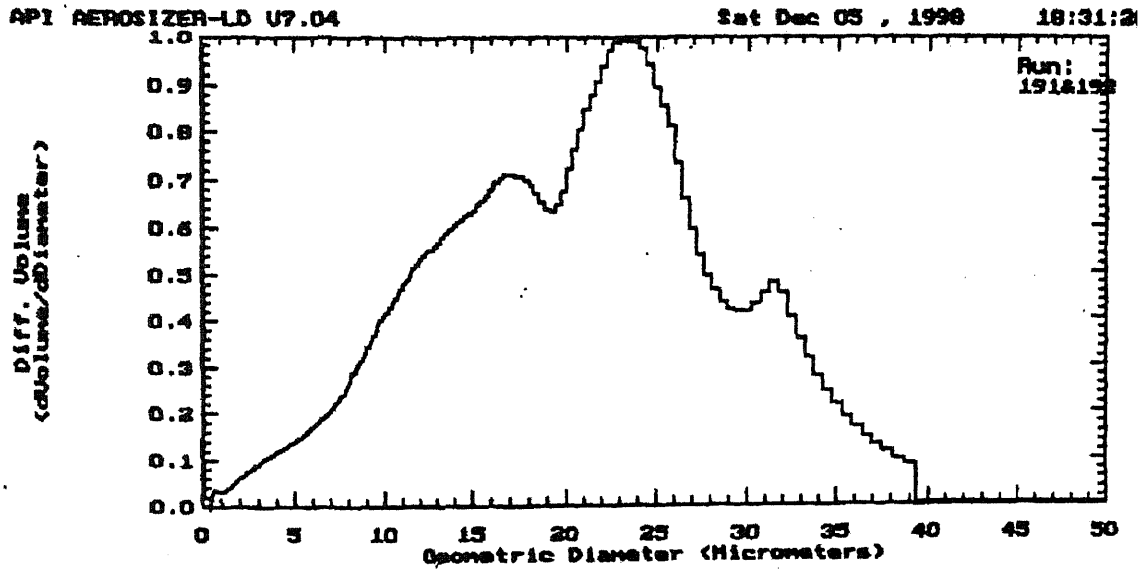


**Figure C3** Aerosizer particle size distribution for the following conditions: Nozzle diameter = 1mm, Pressure = 30psi, Guest = 1.0g, Vessel = 50cc.

***Mean size = 18.94μm*** Disperser type = Pulse jet

Standard Deviation = 1.632 Mode (linear scale) = 23.09

Alumina density = 3.26 g/cc Specific area = 0.115 sq. meter/g

Flow rate range = 1.76 l/min – 2.31 l/min

Concentration = 1.87 X $10^8$ particles / cubic meter (counting efficiency = 1.0)

Mass loading = 5.36 x $10^1$ mg/ cubic meter (counting efficiency = 1.0)

| % under | %size | %under | %size |
|---|---|---|---|
| 5% | 7.726 | 55% | 22.30 |
| 10% | 10.3 | 60% | 23.19 |
| 15% | 12.10 | 65% | 24.08 |
| 20% | 13.66 | 70% | 25.02 |
| 25% | 15.09 | 75% | 26.09 |
| 30% | 16.40 | 80% | 27.51 |
| 35% | 17.64 | 85% | 29.45 |
| 40% | 18.94 | 90% | 31.45 |
| 45% | 20.26 | 95% | 33.75 |
| 50% | 21.34 | | |

*4) Experimental conditions*

Nozzle diameter = 1mm

Aerosolizing pressure = 30psi

Amount of alumina taken in the vessel = 1.0 grams

Pressure vessel capacity = 50cc

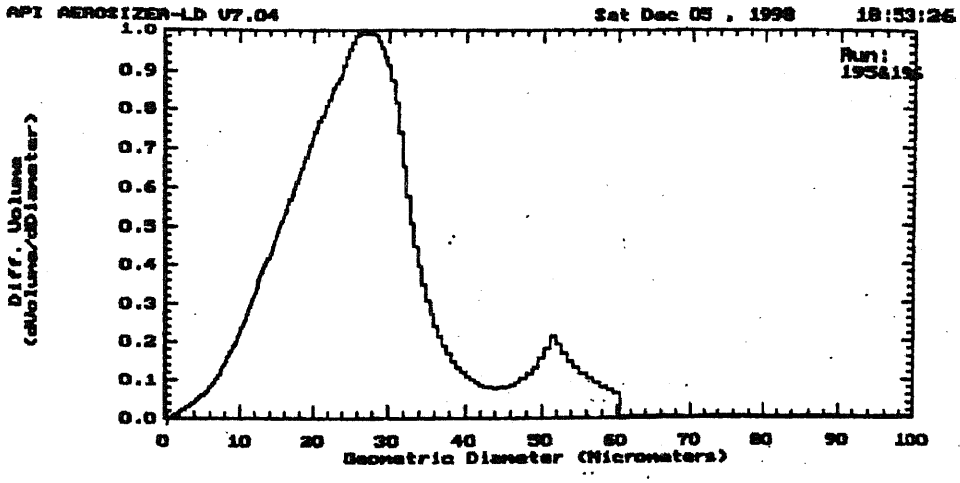


**Figure C4** Aerosizer volumetric particle size distribution for the following conditions: Nozzle diameter = 1mm, Pressure = 30psi, Guest = 1.0g, Vessel = 50cc.

***Mean size = 24.26μm***

Disperser type = Pulse jet

Standard Deviation = 1.567

Mode (linear scale) = 27.76

Alumina density = 3.26 g/cc

Specific area = 0.0857sq. meter/g

Flow rate range = 1.61 l/min – 2.26 l/min

Concentration = 2.65 X $10^8$ particles / cubic meter (counting efficiency = 1.0)

Mass loading = 4.86x $10^2$ mg/ cubic meter (counting efficiency = 1.0)

| % under | %size | %under | %size |
|---|---|---|---|
| 5% | 10.99 | 55% | 26.63 |
| 10% | 13.91 | 60% | 27.68 |
| 15% | 16.06 | 65% | 28.74 |
| 20% | 17.84 | 70% | 29.84 |
| 25% | 19.41 | 75% | 31.04 |
| 30% | 20.82 | 80% | 32.59 |
| 35% | 22.12 | 85% | 35.18 |
| 40% | 23.33 | 90% | 41.79 |
| 45% | 24.49 | 95% | 51.34 |
| 50% | 25.58 | | |

*5) Experimental conditions*

Nozzle diameter = 1mm

Aerosolization pressure = 30psi

Amount of alumina taken in pressure vessel = 1.0 grams

Pressure vessel capacity = 50cc

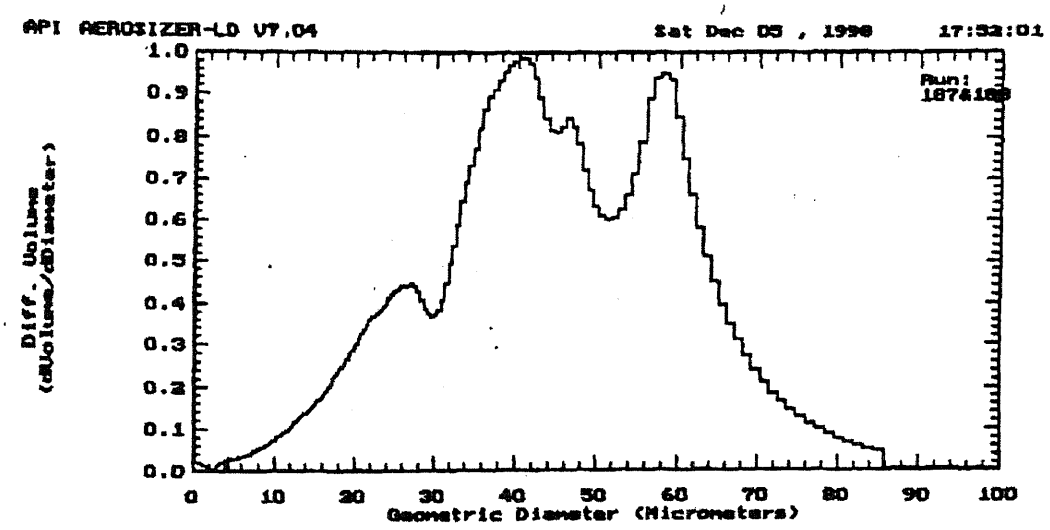


**Figure C5** Aerosizer volumetric particle size distribution for following conditions: Nozzle diameter = 1mm, Pressure = 30psi, Guest = 1.0g, Vessel = 50cc.

***Mean size = 42.11 μm*** Disperser type = Pulse jet

Standard Deviation = 1.524 Mode (linear scale) = 27.76

Alumina density = 3.26 g/cc Specific area = 0.0857sq. meter/g

Flow rate range = 1.80 l/min – 1.92 l/min

Concentration = 5.84 X $10^8$ particles / cubic meter (counting efficiency = 1.0)

Mass loading = 5.08 X $10^2$ mg/ cubic meter (counting efficiency = 1.0)

| % under | %size | %under | %size |
|---|---|---|---|
| 5% | 19.29 | 55% | 47.12 |
| 10% | 24.65 | 60% | 49.60 |
| 15% | 28.47 | 65% | 52.52 |
| 20% | 32.67 | 70% | 55.15 |
| 25% | 35.24 | 75% | 57.19 |
| 30% | 37.28 | 80% | 59.07 |
| 35% | 39.15 | 85% | 61.27 |
| 40% | 40.95 | 90% | 64.41 |
| 45% | 42.84 | 95% | 69.71 |
| 50% | 44.98 | | |

The following table summarizes the average size of aggregates for good de-aggregation and poor de-aggregation conditions.

**Table C.1** Average size of particles during de-aggregation through the nozzle

| | Mean size (μm) | Mean size (μm) | Mean size (μm) | Average size (μm) |
|---|---|---|---|---|
| Good de-aggregation | 0.9543 | 2.116 | _ | 1.54 |
| Poor de-aggregation | 18.94 | 24.26 | 42.11 | 28.44 |

## APPENDIX D

## TABULATION OF COATING RESULTS

Host = Glass beads (500μm)

Guest = Alumina (0.7μm)

**Table D.1** DCPS results for: Nozzle Diameter of 0.3mm, Pressure = 150psi,Vessel capacity of 2000 cc.

| Sl. No. | Wt. of Guest in g | Wt.of empty beaker in g | Beaker + coated host in g | Beaker + De-coated host in g | Wt.of coated host in g | Wt. Of coating in g | Coating Efficiency |
|---|---|---|---|---|---|---|---|
| 1 | 1.0 | 29.612 | 33.151 | 33.116 | 3.539 | 0.035 | 4.994 |
| 2 | 0.7 | 28.602 | 31.182 | 31.148 | 2.580 | 0.034 | 9.538 |
| 3 | 0.7 | 28.586 | 31.390 | 31.339 | 2.804 | 0.051 | 13.232 |
| 4 | 0.3 | 30.398 | 33.739 | 33.765 | 3.337 | 0.034 | 19.047 |
| 5 | 0.3 | 30.402 | 33.739 | 33.765 | 3.337 | 0.034 | 17.156 |
| 6 | 0.1 | 30.536 | 32.895 | 32.890 | 2.359 | 0.005 | 10.620 |

**Table D.2** DCPS results for: Nozzle Diameter = 1mm, Pressure = 150psi, and Vessel capacity of 2000 cc

| Sl. No | Wt. Of guest in g | Wt. Of empty beaker in g | Beaker + coated host in g | Beaker + de-coated host in g | Wt. Of coated host in g | Wt. Of coating in g | Coating Efficiency |
|---|---|---|---|---|---|---|---|
| 1 | 1.5 | 29.602 | 33.134 | 32.843 | 3.535 | 0.291 | 29.920 |
| 2 | 1.0 | 29.612 | 32.457 | 32.390 | 2.845 | 0.067 | 12.059 |
| 3 | 0.7 | 28.594 | 31.283 | 32.229 | 2.689 | 0.054 | 14.638 |
| 4 | 0.3 | 30.407 | 33.371 | 33.337 | 2.964 | 0.034 | 11.604 |
| 5 | 0.15 | 30.402 | 31.890 | 31.885 | 1.483 | 0.005 | 11.276 |

**Table D.3** DCPS coating results for: Nozzle Diameter = 1mm, Pressure = 150 psi, Vessel capacity of 50cc.

| Sl. No | Wt. Of guest in g | Wt. Of empty beaker in g | Beaker + coated host in g | Beaker + de-coated host in g | Wt. Of coated host in g | Wt. Of coating in g | Coating Efficiency |
|---|---|---|---|---|---|---|---|
| 1 | 0.7 | 28.431 | 30.848 | 30.779 | 2.417 | 0.069 | 14.270 |
| 2 | 1.0 | 28.447 | 30.543 | 30.500 | 2.096 | 0.043 | 10.257 |

**Table D.4** DCPS results for: Nozzle Diameter = 1mm, and Vessel capacity = 50cc.

| Sl. No | Psi * | Wt. Of guest in g | Wt. Of empty beaker in g | Beaker + coated host in g | Beaker + de-coated host in g | Wt. Of coated host in g | Wt. Of coating in g | Coating Efficiency |
|---|---|---|---|---|---|---|---|---|
| 1 | 30 | 1.0 | 30.404 | 32.335 | 32.055 | 1.931 | 0.280 | 84.790 |
| 2 | 30 | 1.0 | 28.594 | 30.514 | 30.230 | 1.92 | 0.284 | 86.790 |
| 3 | 30 | 0.7 | 28.580 | 30.747 | 30.548 | 2.167 | 0.199 | 72.227 |
| 4 | 30 | 1.0 | 29.604 | 32.243 | 32.094 | 2.639 | 0.149 | 28.251 |
| 5 | 30 | 1.0 | 28.448 | 30.971 | 30.621 | 2.522 | 0.350 | 69.407 |

* pressure operated at, in psi

Average coating efficiency = 68%

# APPENDIX E

## API AEROSIZER – PARTICLE SIZE ANALYZER

The API Aerosizer technology for particle analysis is based on the aerodynamic technique developed by Dr. Barton Dahnake. The Aerosizer particle measuring system is capable of measuring individually the size of particles in the range of less than 0.2 to 700 micrometers. The particles may be in the form of dry powder, may be suspended in a gas, or may be sprayed from a liquid suspension. The particle size is measured by expanding the air-particle suspension through a nozzle into a partial vacuum. The air leaves the nozzle at near sonic velocity and continues to accelerate through the measurement zone. The particles are accelerated by the drag force generated by the accelerating air stream. Very small particles are accelerated to nearly the air velocity by the drag force between the air and the particles. Large particles experience lower acceleration due to their greater mass. The particle size is measured by time of flight method. The time-of-flight of a particle is measured by generating two beams of laser light through the instrument's measurement zone. As particles pass through the laser beams, they scatter light which is detected and converted into electronic signals by two photomultplier tubes. One photomultplier detects light scattered as the particles pass through the first beam and the other photomultiplier detects when the particles pass through the second beam. The time between the two events (time of flight) is measured with a precision of 25 nanoseconds. The relationship between the particle size and time of flight depends on density of the particle. The relationship has been carefully determined using a combination of theoretical concepts and experimental measurements of particles with accurately known

diameters and densities. The following figure (Figure E1) shows the results of this determination. These results are entered in a computer program and are used to change measurements of the time of flight into particle size and for which density of the particle must be known to permit the conversion.

## E.1 An overview of the Aerosizer

The Aerosizer system consists of four major components as shown in figure below (Figure E2). They are the Sample Presentation Device, Aerosizer Sensor Unit, Vacuum Pump, and the Aerosizer Controller. The sample presentation device is used to introduce the sample in Aerosol form to the Aerosizer. The aerosizer sensor unit contains the hardware and optics necessary to perform the Time-of-flight measurement. The vacuum system generates the necessary air flows and pressures required by the sensor unit as well as collecting the analyzed sample to reduce operator exposure. The aerosizer controller contains the API Data Acquisition hardware and software that communicates with the sensor unit and sample presentation devices as well as collecting and analyzing the Time of flight signals from the sensor unit. More information about the Aerosizer can be obtained from the following source:

Amherst Process Instruments,

Mountain Farms Technology Park,

Hadley, Ma 01035

Phone: 413 586 2744

Fax: 413 585 0536

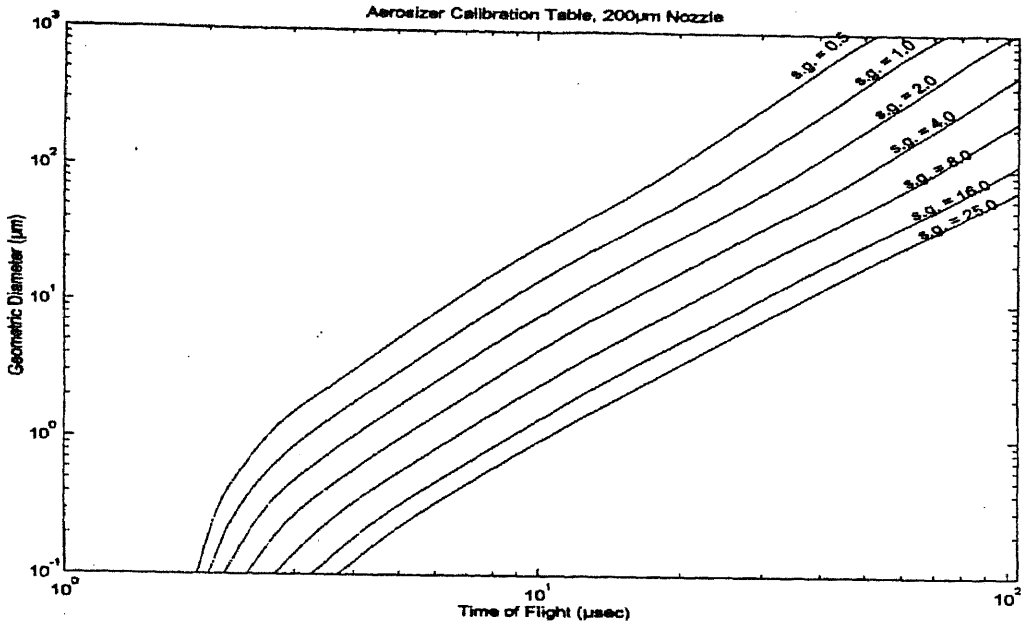


**Figure E1** Aerosizer Calibration table

SYSTEM COMPONENTS

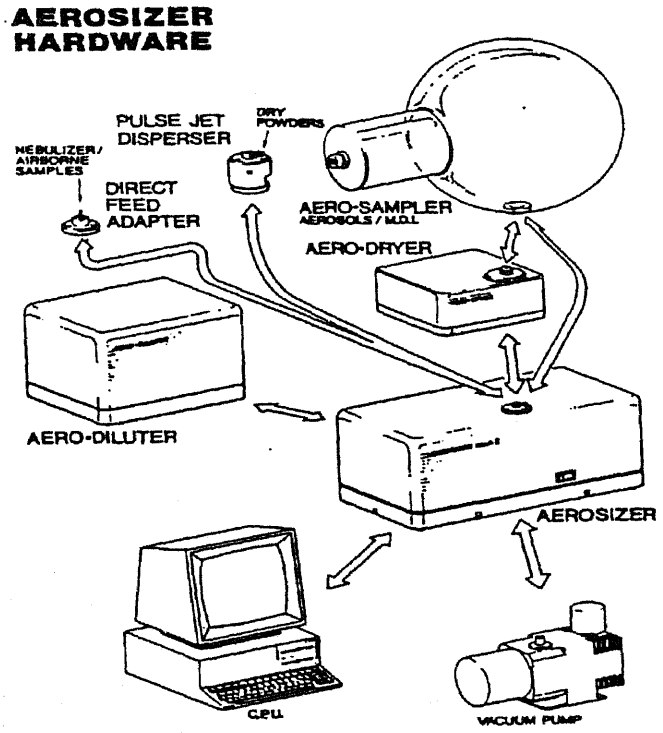


**Figure E2** Aerosizer system components

## APPENDIX F

## EVALUATION OF GUEST-HOST PARTICLE RELATIVE VELOCITY

During the process of coating, the velocity decreases with pressure. The time of release of aerosol is noted for various pressures inside the vessel to evaluate the differential velocity.

Total volume of aerosol = volume of the vessel X (pressure/14.646psi)

$$\text{relative velocity} = \frac{\text{Total volume of aerosol at time } t_1 - \text{total volume of aerosol at time } t_2}{\text{cross section of flow in spouted bed} \times \text{time of release}}$$

Cross-sectional area of flow of aerosol varies with pressure and is assumed at various pressures. At 300 psi pressure, the square cross-sectional area of flow of side 2.5 centimeter is assumed. At 200 psi, the square cross-sectional area of flow of side 2.25 centimeter is assumed. At 100 psi, the square cross-sectional area of flow of side 1.75centimeter is assumed. The volume of the vessel considered is 2000cc.

**Table F.1** Change in aerosol stream velocity with time and pressure

| Sl. No. | Time (s) | Pressure (psi) | Total volume (cc) | Difference in volume | Cross-sectional area of flow (sq. cm) | Differential velocity (cm/s) |
|---|---|---|---|---|---|---|
| 1 | 0 | 300 | 42827.45 | 13609.15 | 6.25 | 49.5 |
| 2. | 44 | 200 | 29218.30 | 13609.15 | 5.06 | 48.9 |
| 3 | 99 | 100 | 15609.15 | 9526.41 | 3.06 | 49.4 |
| 4 | 162 | 30 | 6082.74 | | | |

The gas velocity is found to be constant as its velocity is at the velocity of sound. The product of cross sectional area and velocity, which is the volumetric flow rate, is always a constant. Considering the velocity of aerosol in the spouted bed to be around 50cm/s, the theoretical coating efficiency found for aerosizer evaluated mean particle size of 0.9523 μm and 2.116 μm from equations 3.5 and 3.29 are 55.56% and 130.88% respectively.

# APPENDIX G

# POWDER LOSS IN PRESSURE VESSEL AND PIPING

During the process of aerosolization, the guest particles may sediment in the vessel or in the pipings before being discharged through the nozzle and thus may not be available for the process of de-aggregation, aerosol generation and coating of host particles in the spouted bed. This powder loss due to sedimentation of guest particles depends on size of the aerosolized guest aggregates. If the size of a guest particle is greater than critical guest particle radius, it sediments at the bottom of the vessel and thus would be unavailable for coating. In the following two subsections, we determine the critical guest particle radius for the pressure vessel and for the pipings.

## G.1 Determination of Critical Guest Particle Radius in pressure vessel

Critical settling velocity or falling velocity is the ratio of pressure vessel height to the time of release of aerosol through the nozzle. The height of pressure vessel of capacity 2000cc is 40cm and that of 50cc is 1cm and the time of release depends on the aerosolization pressure.

This appendix demonstrates a sample calculation for tables G.1 and G.2.

For table G1, for

Large vessel capacity = 2000cc.

Aerosolizing pressure = 150psi.

Time of release of aerosol = 315 seconds.

Height of the vessel = 40cm.

$$\text{critical velocity} = \frac{\text{vessel height}}{\text{time of release}} \tag{G.1}$$

$$\text{critical velocity} = \frac{40}{315} = 0.1269 \cong 0.13 \text{cm/s} \tag{G.2}$$

Stokes equation can be used for low Reynolds number;

$$V = \frac{2g\, r_g^2 \rho_g}{9\upsilon} \tag{G.3}$$

$$0.13 = \frac{2 \times 981 \times r_g^2 \times 1.12}{9 \times 1.5 \times 10^{-4}} \tag{G.4}$$

where $\rho_g$ is density of guest particle aggregates = 1.16g/cc

and $\nu$ is the kinematic viscosity = $1.5 \times 10^{-4}$ sq.cm / s.

$$r_g = 2.7921\ \mu \cong 2.79\ \mu$$

Similarly, the calculations are done for other conditions and results are tabulated in table G.1.

**Table G.1** Critical guest particle radius due to sedimentation in pressure vessel

| Sl. No. | Volume of vessel (cc) | Pressure in vessel (psi) | Time of release (s) | Critical falling Velocity (cm/s) | Critical radius (μm) |
|---|---|---|---|---|---|
| 1 | 2000 | 150 | 315 | 0.13 | 2.79 |
| 2 | 2000 | 300 | 470 | 0.09 | 2.29 |
| 3 | 50 | 30 | 25 | 0.04 | 1.57 |
| 4 | 50 | 150 | 90 | 0.01 | 0.88 |

The size of aggregates suspended in the aerosol inside the vessel are larger than the size of the aggregates after de-aggregation through the nozzle. From table G.1 (rows 3,4), we find that if the radius of the guest aggregates is greater than 1.6μm (for small vessel), the majority of particles can sediment inside the small vessel. However, it is found from the aerosizer particle size analysis that the mean size of aggregates of guest particles de-aggregated under low pressures using large diameter nozzle is 28.4μm (Appendix B). Owing to high linear velocity and small cross-sectional area of the vessel, the large aggregates that has sedimented in the vessel are also driven by the fluid stream. For large vessel, if the radius of the aerosolized guest particle is greater than 2.3μm, the guest particles may sediment in the vessel. It is found from Appendix B that the average size of de-aggregated guest particles under high pressures and small diameter nozzle is 1.54μm. The cross-sectional area of the vessel is large and linear velocity inside the vessel is small. As a result the gas velocity is not sufficient to entrain the large aggregates into the stream and thus they can be lost due to sedimentation in the vessel.

## G.2 Determination of Critical Guest Particle Radius in Pipings

If the size of guest aggregates is greater than critical guest particle radius, the aggregates will sediment in the pipings during its flow. The following table F.2 summarizes the guest particle critical radius for various pressures and pressure vessels by using Fuch's monographs, figure 3.2 and sample calculation is illustrated below..

For table G.2, for

Aerosolization pressure = 150psi.

Volume of pressure vessel = 2000cc.

Length of the pipings = 27cm.

Diameter of pipe = ½ inch

$$\text{velocity of flow} = \frac{\text{volumetric flowrate}}{\text{cross-sectional area of pipe}} \tag{G.5}$$

$$\text{velocity of flow} = \frac{2000\left(\frac{150+14.696}{14.696}\right)}{\pi\left(\frac{2.54}{2}\right)^2 \times 315} = 56.17 \tag{G.6}$$

$$\text{sedimentation velocity} = \text{velocity of flow} \times \frac{\text{pipe diameter}}{\text{length of the pipe}} \tag{G.7}$$

$$\text{sedimentation velocity} = 56.17 \times \frac{1.27}{27} = 2.6458\ \text{cm/s} \cong 2.65\text{cm/s}$$

Critical guest particle is found from Fuch's monograph in figure 3.2 for corresponding sedimentation velocity. Critical guest particle radius = 7.07μm. Similarly calculations are done for other experimental conditions and the results are tabulated in table G.2.

**Table G.2** Critical guest particle radius due to sedimentation in piping

| Sl. No. | Volume of vessel (cc) | Aerosolizing pressure (psi) | Velocity in pipe (cm/s) | Sedimentation velocity (s) | log r | r (μm) |
|---|---|---|---|---|---|---|
| 1 | 2000 | 150 | 56.17 | 2.65 | -3.15 | 7.07 |
| 2 | 2000 | 300 | 71.93 | 3.39 | -3.08 | 8.32 |
| 3 | 50 | 30 | 4.80 | 0.23 | -3.40 | 3.98 |
| 4 | 50 | 150 | 15.58 | 0.73 | -3.28 | 5.25 |

From table G.2, we find that the critical radius of guest particle aggregates in the pipings is in the range of 5 - 8μm for coating carried out at high pressures using small diameter nozzle (rows 1,2 and 4). If the size of the aggregates is greater than 5 μm , the particles may sediment in the pipe. However, due to high linear velocity, the particles sedimentation in the pipe may be less.

From table G.2, the critical guest particle radius for de-aggregation under low pressure and large diameter nozzle is around 4 μm ( row 3). If the size of the aggregates is greater than 4 μm, they might sediment in the pipings. From appendix C, the mean size for the same experimental conditions is found to be 28.44μm. Owing to high linear velocity in the pipe, the powder loss in the pipe may be less.

## REFERENCES


1. R. K. Singh, A. Ata, and J. Fitz-Gerald and Ya. I. Rabinovich, " Dry Coating Method using Magnetically Assisted Impaction In a Randomly Turbulent Fluidized Bed," *KONA*, No. 15, 1997, pp. 121-131.

2. X.X. Cheng, *The Studies of Uniformity of Particle Coating in Fluidized Bed,* doctoral dissertation, The College of Engineering of West Virginia University, Morgantown, West Virginia, 1993.

3. J. Kucharski and A.Kmiec, "Hydrodynamics, Heat and Mass Transfer During Coating of Tablets in a Spouted Bed," *Canadian Journal of chemical Engineering*, Vol. 61, Jun. 1983, pp 435-439.

4. J. Kucharski and A. Kmiec, " Kinetics of Granulation Process During Coating of Tablets in a Spouted Bed," *Chemical Engineering Science*, Vol. 44, No. 8, 1989, pp. 1627- 1636.

5. K.A. Nielsen, C.W.Glancy, K.L.Hoy and K.M.Perry, "A Atomization Mechanism for Airless Spraying: The Supercritical Fluid Spray Process," ICLASS-91, Gaithersburg, MD, U.S.A, July 1991, pp 367-374.

6. R.J.Woods and D.C. Busby, "Cost-Effective Coating with Supercritical Fluid Technology," *Environmental Effects*, MP/November 1995, pp 45-48.

7. K.A.Nielsen, J.N.Argryopooulos, D.C.Busby, D.J.Dickson, C.W. Glancy, A.C.Kuo and C.Lee, "Supercritical Fluid Spray Coating: Technical Development of a New Pollution Prevention Technology," *Proc. Water-Borne & Higher Solids, and Powder Coatings Symposium*, New Orleans, LA, U.S.A, feb. 24-26, 1993, pp 173-193.

8. P.G. Debenedetti, J.W.Tom, X.Kwauk, and S.D.Yeo, "Rapid Expansion of Supercritical Solutions (RESS): Fundamentals and Applications," *Fluid Phase Equilibria*, Vol.82, 1993, pp 311-321.

9. M. Ramlakhan, C. Wu, S. Watano, R. Dave and R. Pfeffer, " Dry Particle Coating by Magnetically Assisted Impaction Coating (MAIC) Process," *submitted for publication,* Particle Processing Research Center, New Jersey Institute of Technology, NJ 07102-1982

10. H. Kage, T. Takahashi, T. Yoshida, H.Ogura, Y. Matsuno, "Coating Efficiency of seed particles in a fluidized bed by atomization of a powder suspension," *Powder Technology*, Vol. 86, 1996, pp 243-250.

11. H.Kage, T.Takahashi, M.Fujiyama and Y.Matsuno, "Powder Coating of Particles in Fluidized Bed Granulator," *Proc. of Asian Conference on Fluidized Bed and Three-phase Reactors,* Tokyo, Japan, 1988, pp. 322.

12. H. Honda, M.Kimura, T.Matsuno and M.Koishi, "Preparation of Composite and Encapsulated Powder Particles by Dry Impact Blending," *Research Paper, Chimicaoggi* – june 1991.

13. E. Abe, H. Hirosue and N. Yamada, "Coating of Seed Particles in a Tumbling Fluidized Bed by Atomizing the Slurries of Clayey Particles – Coating Efficiency and Growth Rate," *Proc. of World Congress III on Powders and Aerosol Properties & Powder Technology,* Tokyo, Japan, 1986.

14. H.Honda, M.Kimura, F.Honda, T.Matsuno and M.Koishi, "Preparation of monolayer particle coated powder by the dry impact blending process utilizing mechanochemical treatment," *Colloids and Surfaces A: Physiochemical and Engineering Aspects*, Vol. 82, 1994, pp 117-128.

15. M.A. Gamez, A Fundamental Study on the Coating of Powders, doctoral dissertation, *College of Engineering, University of Osaka Prefecture*, Japan, Jan. 1991.

16. Y.Endo, S.Hasebe, Y.Kousaka, "Dispersion of aggregates of fine powder by acceleration in an air stream and its application to the evaluation of adhesion between particles," *Powder Technology*, Vol. 91, 1997, pp 25-30.

17. H.Amit, De-aggregation of Particles by Depressurization, master's thesis, Dept.of Environmental Engineering, New Jersey Institute of Technology, Newark, NJ, 1999.

18. J.G.Knudsen and D.L.Katz, *Fluid Dynamics and Heat Transfer*, McGraw-Hill, N.Y., Toronto & London 1979, pp 235.

19. S.S.Dukhin, G.Kretzschmar, R.Miller, *Dynamics of Adsorption on Liquid Interfaces*, Elsevier, Paris, 1996.

20. N.A. Fuchs, *The Mechanics of Aerosols,* A Pergamon Press, Mac Millan company, New York, 1964.

21. W.L. McCabe, J.C.Smith, D.Harriott, *Unit Operations of Chemical Engineering*, McGraw-Hill, N.Y., 1978, pp 154.

22. J.F.Davidson and D.Harrison, *Fluidization*, Academic Press, London & NY, 1971.

23. S. Wall, W. John, H. Wang, "Measurements of Kinetic Energy Loss for Particles Impacting Surfaces," *Aerosol Science and Technology*, Vol. 12, 1990, pp 926-946.